An Observational Perspective of Transitional Disks

Catherine Espaillat
Boston University

James Muzerolle
Space Telescope Science Institute

Joan Najita
National Optical Astronomy Observatory

Sean Andrews
Harvard-Smithsonian Center for Astrophysics

Zhaohuan Zhu
Princeton University

Nuria Calvet
University of Michigan

Stefan Kraus
University of Exeter

Jun Hashimoto
The University of Oklahoma

Adam Kraus
University of Texas

Paola D'Alessio
Universidad Nacional Autónoma de México

Transitional disks are objects whose inner disk regions have undergone substantial clearing. The *Spitzer Space Telescope* produced detailed spectral energy distributions (SEDs) of transitional disks that allowed us to infer their radial dust disk structure in some detail, revealing the diversity of this class of disks. The growing sample of transitional disks also opened up the possibility of demographic studies, which provided unique insights. There now exist (sub)millimeter and infrared images that confirm the presence of large clearings of dust in transitional disks. In addition, protoplanet candidates have been detected within some of these clearings. Transitional disks are thought to be a strong link to planet formation around young stars and are a key area to study if further progress is to be made on understanding the initial stages of planet formation. Here we provide a review and synthesis of transitional disk observations to date with the aim of providing timely direction to the field, which is about to undergo its next burst of growth as ALMA reaches its full potential. We discuss what we have learned about transitional disks from SEDs, color-color diagrams, and imaging in the (sub)mm and infrared. We note the limitations of these techniques, particularly with respect to the sizes of the clearings currently detectable, and highlight the need for pairing broad-band SEDs with multi-wavelength images to paint a more detailed picture of transitional disk structure. We review the gas in transitional disks, keeping in mind that future observations with ALMA will give us unprecedented access to gas in disks, and also observed infrared variability pointing to variable transitional disk structure, which may have implications for disks in general. We then distill the observations into constraints for the main disk clearing mechanisms proposed to date (i.e., photoevaporation, grain growth, and companions) and explore how the expected observational signatures from these mechanisms, particularly planet-induced disk clearing, compare to actual observations. Lastly, we discuss future avenues of inquiry to be pursued with ALMA, JWST, and next generation of ground-based telescopes.

1. INTRODUCTION

Disks around young stars are thought to be the sites of planet formation. However, many questions exist concerning how the gas and dust in the disk evolve into a planetary system. Observations of T Tauri stars (TTS) may provide insights into these questions, and a subset of TTS, the "transitional disks," have gained increasing attention in this regard. The unusual SEDs of transitional disks (which feature infrared excess deficits) may indicate that they have developed significant radial structure.

Transitional disk SEDs were first identified by *Strom et al.* (1989); *Skrutskie et al.* (1990) from near-infrared (NIR) ground-based photometry and IRAS mid-infrared (MIR) photometry. These systems exhibited small NIR and/or MIR excesses, but significant mid- and far-IR (FIR) excesses indicating that the *dust* distribution of these disks had an inner hole (i.e., a region that is mostly devoid of small dust grains from a radius R_{hole} down to the central star). They proposed that these disks were in transition from objects with optically thick disks that extend inward to the stellar surface (i.e., Class II objects) to objects where the disk has dissipated (i.e., Class III objects), possibly as a result of some phase of planet formation. A few years later, *Marsh and Mahoney* (1992, 1993) proposed that such transitional disk SEDs were consistent with the expectations for a disk subject to tidal effects exerted by companions, either stars or planets.

More detailed studies of transitional disks became possible as increasingly sophisticated instruments became available. The spectrographs on board *ISO* were able to study the brightest stars and *Bouwman et al.* (2003) inferred a large hole in the disk of the Herbig Ae/Be star HD 100546 based on its SED. Usage of the term "transitional disk" gained substantial momentum in the literature after the *Spitzer Space Telescope*'s (*Werner et al.* 2004) Infrared Spectrograph (IRS; *Houck et al.* 2004) was used to study disks with inner holes (e.g., *D'Alessio et al.* 2005; *Calvet et al.* 2005). *Spitzer* also detected disks with an annular "gap" within the disk as opposed to holes (e.g., *Brown et al.* 2007; *Espaillat et al.* 2007). In this review, we use the term *transitional disk* to refer to an object with an inner disk hole and *pre-transitional disk* to refer to a disk with a gap. For many (pre-)transitional disks, the inward truncation of the outer dust disk has been confirmed, predominantly through (sub)millimeter interferometric imaging (e.g., *Hughes et al.* 2007; *Brown et al.* 2008; *Hughes et al.* 2009; *Brown et al.* 2009; *Andrews et al.* 2009; *Isella et al.* 2010b; *Andrews et al.* 2011b). We note that (sub)mm imaging is not currently capable of distinguishing between a hole or gap in the disk (i.e., it can only detect a generic region of clearing or a "cavity" in the disk). Also, it has not yet been confirmed if these clearings detected in the dust disk are present in the gas disk as well. The combination of these dust cavities with the presence of continuing gas accretion onto the central star is a challenge to theories of disk clearing.

The distinct SEDs of (pre-)transitional disks have lead many researchers to conclude that these objects are being caught in an important phase in disk evolution. One possibility is that these disks are forming planets given that cleared disk regions are predicted by theoretical planet formation models (e.g., *Paardekooper and Mellema* 2004; *Zhu et al.* 2011; *Dodson-Robinson and Salyk* 2011). Potentially supporting this, there exist observational reports of protoplanet candidates in (pre-)transitional disks (e.g., LkCa 15, T Cha; *Kraus et al.* 2011; *Huélamo et al.* 2011). Stellar companions can also clear the inner disk (*Artymowicz and Lubow* 1994) but many stars harboring (pre-)transitional disks are single stars (*Kraus et al.* 2011). Even if companions are not responsible for the clearings seen in all (pre-)transitional disks, these objects still have the potential to inform our understanding of how disks dissipate, primarily by providing constraints for disk clearing models involving photoevaporation and grain growth.

In this chapter, we will review the key observational constraints on the dust and gas properties of (pre-)transitional disks and examine these in the context of theoretical disk clearing mechanisms. In §2, we look at SEDs (§ 2.1) as well as (sub)mm (§ 2.2) and IR (§ 2.3) imaging. We also review IR variability in (pre-)transitional disks (§ 2.4) and gas observations (§ 2.5). In §3, we turn the observations from §2 into constraints for the main disk clearing mechanisms proposed to date (i.e., photoevaporation, grain growth, and companions) and discuss these mechanisms in light of these constraints. In §4, we examine the demographics of (pre-)transitional disks (i.e., frequencies, timescales, disk masses, accretion rates, stellar properties) in the context of disk clearing and in §5 we conclude with possibilities for future work in this field.

2. OVERVIEW OF OBSERVATIONS

In the two decades following *Strom et al.* (1989)'s identification of the first transitional disks using NIR and MIR photometry, modeling of the SEDs of these disks, enabled largely by *Spitzer* IRS, inferred the presence of holes and gaps that span several AU (§ 2.1). Many of these cavities were confirmed by (sub)mm interferometric imaging (§ 2.2) and IR polarimetric and interferometric (§ 2.3) images. Later on, MIR variability was detected which pointed to structural changes in these disks (§ 2.4). While there are not currently as many constraints on the gas in the disk as there are for the dust, it is apparent that the nature of gas in the inner regions of (pre-)transitional disks differs from other disks (§ 2.5). These observational results have significant implications for our understanding of planet formation and we review them in the following sections.

2.1 Spectral Energy Distributions

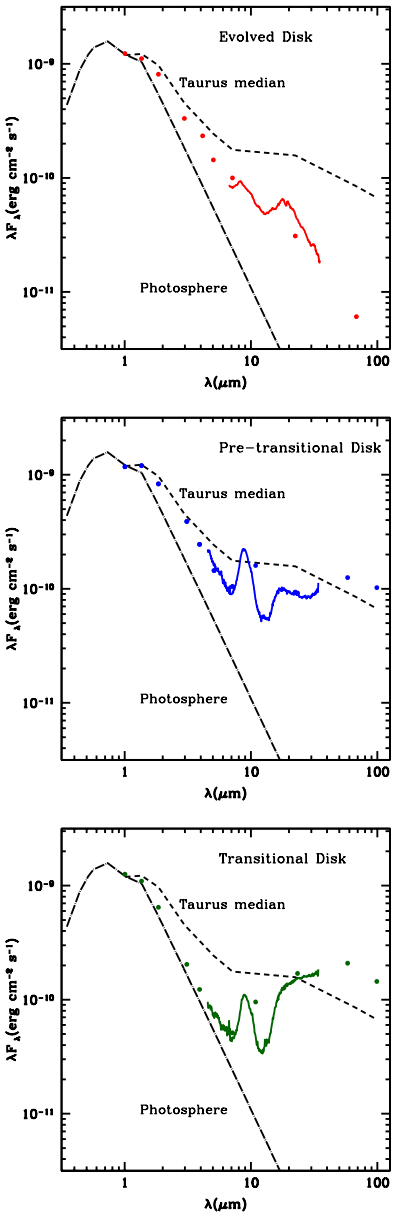

Fig. 1.— SEDs of an evolved disk (top; RECX 11; *Ingleby et al.* 2011), a pre-transitional disk (middle; LkCa 15; *Espaillat et al.* 2007), and a transitional disk (bottom; GM Aur; *Calvet et al.* 2005). The stars are all K3-K5 and the fluxes have been corrected for reddenning and scaled to the stellar photosphere (dot-long-dashed line) for comparison. Relative to the Taurus median (short-dashed line; *D'Alessio et al.* 1999), an evolved disk has less emission at all wavelengths, a pre-transitional disk has a MIR deficit (5–20 μm, ignoring the 10 μm silicate emission feature), but comparable emission in the NIR (1–5 μm) and at longer wavelengths, and a transitional disk has a deficit of emission in the NIR and MIR with comparable emission at longer wavelengths.

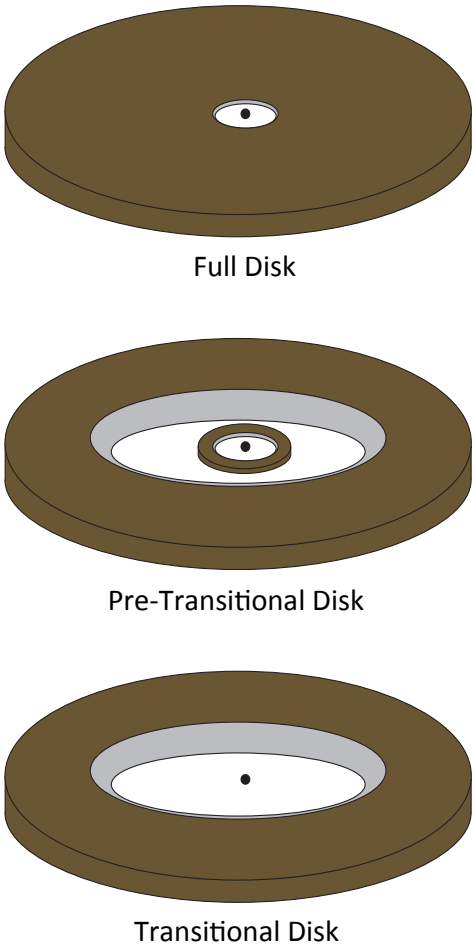

Fig. 2.— Schematic of full (top), pre-transitional (middle), and transitional (bottom) disk structure. For the full disk, progressing outward from the star (black) is the inner disk wall (light gray) and outer disk (dark gray). Pre-transitional disks have an inner disk wall (light gray) and inner disk (dark gray) followed by a disk gap (white), then the outer disk wall (light gray) and outer disk (dark gray). The transitional disk has an inner disk hole (white) followed by an outer disk wall (light gray) and outer disk (dark gray).

SEDs are a powerful tool in disk studies as they provide information over a wide range of wavelengths, tracing different emission mechanisms and material at different stellocentric radii. In a SED, one can see the signatures of gas accretion (in the ultraviolet; see PPIV review by *Calvet et al.* 2000), the stellar photosphere (typically $\sim$1 μm in TTS), and the dust in the disk (in the IR and longer wavelengths). However, SEDs are not spatially resolved and this information must be supplemented by imaging, ideally at many wavelengths (see § 2.2–2.3). Here we review what has been learned from studying the SEDs of (pre-)transitional disks, particularly using *Spitzer* IRS, IRAC, and MIPS.

SED classification

A popular method of identifying transitional disks is to compare individual SEDs to the median SED of disks in the Taurus star-forming region (Fig. 1, dashed line in panels). The median Taurus SED is typically taken as representative of an optically thick full disk (i.e., a disk with no significant radial discontinuities in its dust distribution). The NIR emission (1–5 μm) seen in the SEDs of full disks is dom-

inated by the "wall" or inner edge of the dust disk. This wall is located where there is a sharp change at the radius at which the dust destruction temperature is reached and dust sublimates. TTS in Taurus have NIR excess emission which can be fit by blackbodies with temperatures within the observed range of dust sublimation temperatures (1000–2000 K; *Monnier and Millan-Gabet* 2002), indicating that there is optically thick material located at the dust destruction radius in full disks (*Muzerolle et al.* 2003). Roughly, the MIR emission in the SED traces the inner tens of AU in disks and emission at longer wavelengths comes from outer radii of the disk.

The SEDs of transitional disks are characterized by NIR (1–5 μm) and MIR emission (5–20 μm) similar to that of a stellar photosphere, while having excesses at wavelengths $\sim$20 μm and beyond comparable to the Taurus median, (Fig. 1, bottom; *Calvet et al.* 2005). From this we can infer that the small, hot dust that typically emits at these wavelengths in full disks has been removed and that there is a large hole in the inner disk, larger than can be explained by dust sublimation (Fig. 2, bottom). Large clearings of dust in the submm regime have been identified in disks characterized by this type of SED (§ 2.2; e.g., *Hughes et al.* 2009; *Brown et al.* 2009; *Andrews et al.* 2011b), confirming the SED interpretation. We note that disks with holes have also been referred to as cold disks (*Brown et al.* 2007) or weak excess transitional disks (*Muzerolle et al.* 2010), but here we use the term "transitional disks."

A subset of disks with evidence of clearing in the submm show significant NIR excesses relative to their stellar photospheres, in some cases comparable to the median Taurus SED, but still exhibit MIR dips and substantial excesses beyond $\sim$20 μm (Fig. 1, middle). This NIR excess is blackbody-like with temperatures expected for the sublimation of silicates (*Espaillat et al.* 2008b), similar to the NIR excesses in full disks discussed earlier. This similarity indicates that these disks still have optically thick material close to the star, possibly a remnant of the original inner disk, and these gapped disks have been dubbed pre-transitional disks (*Espaillat et al.* 2007), cold disks (*Brown et al.* 2007), or warm transitional disks (*Muzerolle et al.* 2010). Here we adopt the term "pre-transitional disks" for these objects. In Table 1 we summarize some of properties of many of the well-known (pre-)transitional disks.

We note that some SEDs have emission that decreases steadily at all wavelengths (Fig. 1, top). These disks have been called a variety of names: anemic (*Lada et al.* 2006), homologously depleted (*Currie and Sicilia-Aguilar* 2011), evolved (*Hernández et al.* 2007b, 2008, 2010), weak excess transition (*Muzerolle et al.* 2010). Here we adopt the terminology "evolved disk" for this type of object. Some researchers include these objects in the transitional disk class. However, these likely comprise a heterogenous class of disks, including cleared inner disks, debris disks (see chapter in this volume by *Matthews et al.*), and disks with significant dust grain growth and settling. This has been an issue in defining this subset of objects. We include evolved disks in this review for completeness, but focus on disks with more robust evidence for disk holes and gaps.

Model fitting

Detailed modeling of many of the above-mentioned SEDs has been performed in order to infer the structure of these disks. SEDs of transitional disks (i.e., objects with little or no NIR and MIR emission) have been fit with models of inwardly truncated optically thick disks (e.g., *Rice et al.* 2003; *Calvet et al.* 2002). The inner edge or "wall" of the outer disk is frontally illuminated by the star, dominating most of the emission seen in the IRS spectrum, particularly from $\sim$20–30 μm. Some of the holes in transitional disks are relatively dust-free (e.g., DM Tau) while SED model fitting indicates that others with strong 10 μm silicate emission have a small amount of optically thin dust within their disk holes to explain this feature (e.g., GM Aur; *Calvet et al.* 2005). Beyond $\sim$40 μm, transitional disks have a contribution to their SEDs from the outer disk. In pre-transitional disks, the observed SED can be fit with an optically thick inner disk separated by an optically thin gap from an optically thick outer disk (e.g., *Brown et al.* 2007; *Espaillat et al.* 2007; *Mulders et al.* 2010; *Dong et al.* 2012). There is an inner wall located at the dust sublimation radius which dominates the NIR (2–5 μm) emission and should cast a shadow on the outer disk (see § 2.4). In a few cases, the optically thick inner disk of pre-transitional disks has been confirmed using NIR spectra (*Espaillat et al.* 2010) following the methods of *Muzerolle et al.* (2003). Like the transitional disks, there is evidence for relatively dust-free gaps (e.g., UX Tau A) as well as gaps with some small, optically thin dust to explain strong 10 μm silicate emission features (e.g., LkCa 15; *Espaillat et al.* 2007). The SEDs of evolved disks can be fit with full disk models (*Sicilia-Aguilar et al.* 2011), particularly in which the dust is very settled towards the midplane (e.g., *Espaillat et al.* 2012).

There are many degeneracies to keep in mind when interpreting SED-based results. First, there is a limit to the gap sizes that can be detected with *Spitzer* IRS. Over 80% of the emission at 10 μm comes from within 1 AU in the disk (e.g., *D'Alessio et al.* 2006). Therefore, *Spitzer* IRS is most sensitive to clearings in which a significant amount of dust located at radii $<$1 AU has been removed, and so it will be easier to detect disks with holes (i.e., transitional disks) as opposed to disks with gaps (i.e., pre-transitional disks). The smallest gap in the innermost disk that will cause a noticeable "dip" in the *Spitzer* spectrum would span $\sim$0.3-4 AU. It would be very difficult to detect gaps whose inner boundary is outside of 1 AU (e.g., a gap spanning 5–10 AU in the disk; *Espaillat et al.* 2010). Therefore, with current data we cannot exclude that any disk currently thought to be a full disk contains a small gap nor can we exclude that currently known (pre-)transitional disks have additional clearings at larger radii (e.g., *Debes et al.* 2013). It will be largely up to *ALMA* and the next generation of IR interferometers to detect such small disk gaps (e.g., *de Juan Ovelar et al.* 2013).

TABLE 1
OVERVIEW OF SELECTED (PRE-)TRANSITIONAL DISKS

Object	Class[a]	Submm Cavity Radius (AU)	NIR Cavity detected?	0.1 $M_\odot$ Companion Detection Limit	Accretion Rate ($M_\odot\ yr^{-1}$)	References[b]
AB Aur	PTD	70	...	6 AU	1.3×10^{-7}	1, 25, 38
CoKu Tau/4	TD	...	...	binary[d]	$<10^{-10}$	26, 39
DM Tau	TD	19	...	6 AU	2.9×10^{-9}	2, 25, 40
GM Aur	TD	28	yes	6 AU	9.6×10^{-9}	2, 11, 25, 40
HD 100546	PTD	...	yes	...	5.9×10^{-8}	12, 41
HD 141569	PTD	...	yes	...	7.4×10^{-9}	13, 38
HD 142527	PTD	140	yes	binary[e]	9.5×10^{-8}	3, 14, 27, 38
HD 169142	PTD	...	yes	...	9.1×10^{-9}	15, 38
IRS 48	TD[c]	60	...	8 AU	4.0×10^{-9}	4, 28, 38
LkCa 15	PTD	50	yes	6 AU	3.1×10^{-9}	2, 16, 25, 40
MWC 758	PTD	73	...	28 AU	4.5×10^{-8}	2, 29, 38
PDS 70	PTD	...	yes	6 AU	$<10^{-10}$	17, 30, 42
RX J1604-2130	TD	70	yes	6 AU	$<10^{-10}$	5, 18, 31
RX J1615-3255	TD	30	no	8 AU	4×10^{-10}	2, 19, 33, 43
RX J1633-2442	TD	25	...	6 AU	1.3×10^{-10}	6, 25, 44
RY Tau	PTD	14	...	6 AU	$6.4\text{–}9.1\times10^{-8}$	7, 25, 45
SAO 206462	PTD	46	...	25 AU	4.5×10^{-9}	2, 32, 38
SR 21	TD	36	no	8 AU	$<1.4\times10^{-9}$	2, 20, 33, 46
SR 24 S	PTD	29	...	8 AU	7.1×10^{-8}	2, 33, 46
Sz 91	TD	65	yes	25 AU	1.4×10^{-9}	8, 21, 34
TW Hya	TD	4	no	3 AU	1.8×10^{-9}	9, 22, 35, 40
UX Tau A	PTD	25	...	6 AU	1.1×10^{-9}	2, 25, 40, 47
V4046 Sgr	TD	29	...	binary[f]	5.0×10^{-9}	10, 36, 48
DoAr 44	PTD	30	no	8 AU	3.7×10^{-9}	2, 23, 33, 38
LkH_α 330	PTD	68	no	8 AU	2.2×10^{-8}	2, 24, 33, 38
WSB 60	PTD	15	...	25 AU	3.7×10^{-9}	2, 37, 46

[a]We classify objects as either a pre-transitional disk (PTD) or transitional disk (TD).

[b]Submm cavity radii are from (1) *Piétu et al.* (2005); (2) *Andrews et al.* (2011b); (3) *Casassus et al.* (2012); (4) *Bruderer et al.* (2014); (5) *Mathews et al.* (2012); (6) *Cieza et al.* (2012); (7) *Isella et al.* (2010a); (8) *Tsukagoshi et al.* (2013); (9) *Hughes et al.* (2007); (10) *Rosenfeld et al.* (2013). NIR cavities are from (11) *Hashimoto et al.*, in prep.; (12) *Tatulli et al.* (2011); (13) *Weinberger et al.* (1999); (14) *Avenhaus et al.* (2014); (15) *Quanz et al.* (2013b); (16) *Thalmann et al.* (2010); (17) *Hashimoto et al.* (2012); (18) *Mayama et al.* (2012); (19) *Kooistra et al.*, in prep.; (20) *Follette et al.* (2013); (21) *Tsukagoshi et al.* (2013); (22) *Akiyama et al.*, in prep.; (23) *Kuzuhara et al.*, in prep.; (24) *Bonnefoy et al.*, in prep. Companion detection limits are from (6); (25) *Kraus et al.* (2011); (26) *Ireland and Kraus* (2008); (27) *Biller et al.* (2012); (28) *Lacour et al.*, in prep.; (29) *Grady et al.* (2013); (30) *Kenworthy et al.*, in prep.; (31) *Kraus et al.* (2008); (32) *Vicente et al.* (2011); (33) *Ireland et al.*, in prep.; (34) *Romero et al.* (2012); (35) *Evans et al.* (2012); (36) *Stempels and Gahm* (2004); (37) *Ratzka et al.* (2005). Accretion rates are from (5); (38) *Salyk et al.* (2013); (39) *Cohen and Kuhi* (1979); (40) *Ingleby et al.* (2013); (41) *Pogodin et al.* (2012); (42) *Dong et al.* (2012); (43) *Krautter et al.* (1997); (44) *Cieza et al.* (2010); (45) *Calvet et al.* (2004); (46) *Natta et al.* (2006); (47) *Alcalá et al.* (2014); (48) *Donati et al.* (2011).

[c]The classification of IRS 48 as a TD or PTD is uncertain due the presence of strong PAH emission in this object.

[d]The CoKu Tau/4 binary has a separation of 8 AU, which is within the range of semi-major axes required by tidal interaction theory to explain the 14 AU SED-inferred inner disk hole of this object (*Nagel et al.* 2010). A binary system with an eccentricity of 0.8 can clear out a region 3.5 times the semi-major axis (e.g., *Artymowicz and Lubow* 1994).

[e]The HD 142527 binary is separated by 13 AU. This is not large enough to explain the disk gap. Note that *Casassus et al.* (2013) have disputed the presence of a companion, but recent results from *Close et al.* (2014) may confirm it.

[f]The V4046 Sgr binary has a separation of 0.045 AU, too small to clear out the disk hole. *Rosenfeld et al.* (2013) provide an aperture masking companion limit that suggests there are no 0.1 $M_\odot$ companions down to 3 AU.

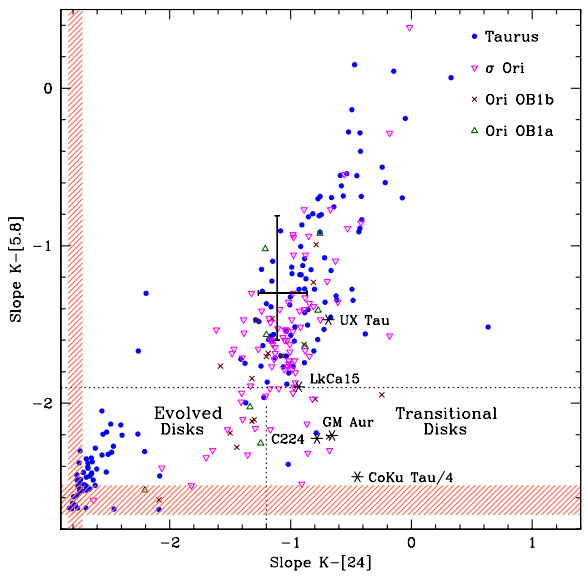

Fig. 3.— *Spitzer* color-color diagram of objects in different associations and clusters. Observations are shown for populations of different ages: Taurus, 1-2 Myr (*Luhman et al.* 2010); σ Ori, 3 Myr (*Hernández et al.* 2007a); Ori OB1b, 7 Myr; Ori OB1a, 10 Myr (*Hernández et al.* 2007b). The hatched region corresponds to stellar photospheric colors. The error bars represent the median and quartiles of Taurus objects (i.e., where most full disks are expected to lie). Well characterized transitional disks (GM Aur, CoKu Tau/4, CVSO224; *Espaillat et al.* 2008a) and pre-transitional disks (LkCa 15, UX Tau) are indicated with asterisks. The dotted lines correspond to the lower quartile of disk emission in σ Ori, and roughly separate the evolved disks (lower left) from the transitional disks (lower right). Note that the pre-transitional disks do not lie below the dotted line, highlighting that it is harder to identify disk gaps based on colors alone. Figure adapted from *Hernández et al.* (2007b).

One should also keep in mind that millimeter data are necessary to break the degeneracy between dust settling and disk mass (see *Espaillat et al.* 2012). Also, the opacity of the disk is controlled by dust and in any sophisticated disk model the largest uncertainty lies in the adopted dust opacities. We will return to disk model limitations in § 2.2.

Implications for color-color diagrams

Another method of identifying transitional disks is through color-color diagrams (Fig. 3). This method grew in usage as more *Spitzer* IRAC and MIPS data became available and (pre-)transitional disks well characterized by *Spitzer* IRS spectra could be used to define the parameter space populated by these objects. In these diagrams, transitional disks are distinct from other disks since they have NIR colors or slopes (generally taken between two IRAC bands, or K and an IRAC band) significantly closer to stellar photospheres than other disks in Taurus, but MIR colors (generally taken between K or one IRAC band and MIPS [24]) comparable or higher than other disks in Taurus (e.g., *Hernández et al.* 2007a, 2008, 2010; *Merín et al.* 2010; *Muzerolle et al.* 2010; *Luhman et al.* 2010; *Williams and Cieza* 2011; *Luhman and Mamajek* 2012). Color-color diagrams are limited in their ability to identify pre-transitional disks because their fluxes in the NIR are comparable to many other disks in Taurus. IRS data can do a better job of identifying pre-transitional disks using the equivalent width of the 10 μm feature or the NIR spectral index (e.g., n_{2-6}) versus the MIR spectral index (e.g., n_{13-31} *Furlan et al.* 2011; *McClure et al.* 2010; *Manoj et al.* 2011). Evolved disks are easier to identify in color-color diagrams since they show excesses over their stellar photospheres that are consistently lower than most disks in Taurus, both in the near *and* mid-IR.

In the future, *JWST*'s sensitivity will allow us to expand *Spitzer*'s SED and color-color work to many more disks, particularly to fainter objects in older and farther star-forming regions, greatly increasing the known number of transitional, pre-transitional, and evolved disks. Upcoming high-resolution imaging surveys with (sub)mm facilities in the near-future (i.e., ALMA) and IR interferometers further in the future (i.e., VLT/MATISSE) will give us a better understanding of the small-scale spatial structures in disks which SEDs cannot access.

2.2 Submillimeter/Radio Continuum Imaging

The dust continuum at (sub)millimeter/radio wavelengths is an ideal probe of cool material in disks. At these wavelengths, dust emission dominates over the contribution from the stellar photosphere, ensuring that contrast limitations are not an issue. Moreover, interferometers give access to the emission structure on a wide range of spatial scales, and will soon provide angular resolution that regularly exceeds 100 mas. The continuum emission at these long wavelengths is also thought to have relatively low optical depths, meaning the emission morphology is sensitive to the density distribution of mm and cm-sized grains (*Beckwith et al.* 1990). These features are especially useful for observing the dust-depleted inner regions of (pre-)transitional disks, as will be illustrated in the following subsections.

(Sub)mm disk cavities

With sufficient resolution, the (sub)mm dust emission from disks with cavities exhibits a "ring"-like morphology, with limb-brightened ansae along the major axis for projected viewing geometries. In terms of the actual measured quantity, the interferometric visibilities, there is a distinctive oscillation pattern (effectively a Bessel function) where the first "null" is a direct measure of the cavity dimensions (see *Hughes et al.* 2007).

As of this writing, roughly two dozen disk cavities have been directly resolved at (sub)mm wavelengths. A gallery of representative continuum images, primarily from observations with the Submillimeter Array (SMA), is shown in

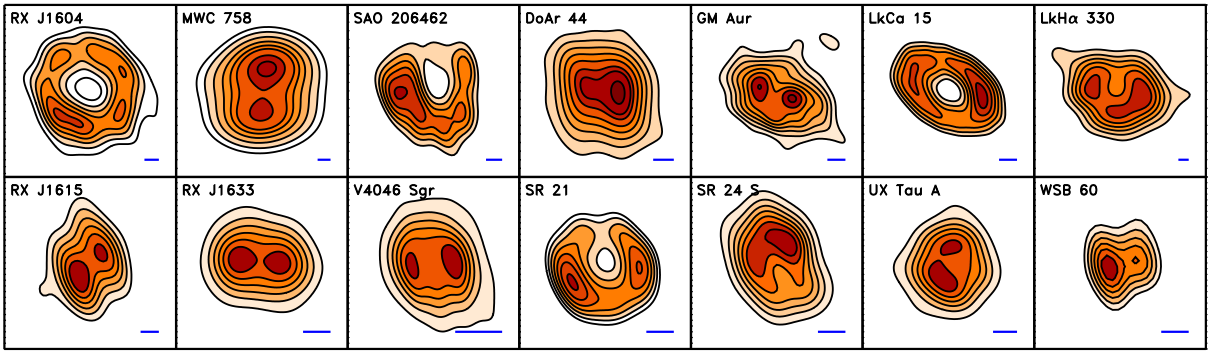

Fig. 4.— A gallery of 880 μm dust continuum images from the Submillimeter Array for (pre-)transitional disks in nearby star-forming regions. From left to right, the panels show the disks around RX J1604.3−2130 (*Mathews et al.* 2012), MWC 758 (*Isella et al.* 2010b), SAO 206462 (*Brown et al.* 2009), DoAr 44 (*Andrews et al.* 2009), GM Aur (*Hughes et al.* 2009), LkCa 15 (*Andrews et al.* 2011b), LkHα 330 (*Brown et al.* 2008), RX J1615.3−3255 (*Andrews et al.* 2011b), RX J1633.9−2442 (*Cieza et al.* 2012), V4046 Sgr (*Rosenfeld et al.* 2013), SR 21 (*Brown et al.* 2009), SR 24 S (*Andrews et al.* 2010), UX Tau A (*Andrews et al.* 2011b), and WSB 60 (*Andrews et al.* 2009). A projected 30 AU scale bar is shown in blue at the lower right corner of each panel.

Fig. 4. For the most part, these discoveries have been haphazard: some disks were specifically targeted based on their infrared SEDs (§ 2.1; e.g., *Brown et al.* 2009), while others were found serendipitously in high resolution imaging surveys aimed at constraining the radial distributions of dust densities (e.g., *Andrews et al.* 2009).

Perhaps the most remarkable aspect of these searches is the frequency of dust-depleted disk cavities at (sub)mm wavelengths, especially considering that the imaging census of all disks has so far been severely restricted by both sensitivity and resolution limitations. In the nearest star-forming regions accessible to the northern hemisphere (Taurus and Ophiuchus), only about half of the disks in the bright half of the mm luminosity ($\sim$disk mass) distribution have been imaged with sufficient angular resolution ($\sim 0.3''$) to find large ($>$20 AU in radius) disk cavities (*Andrews et al.* 2009, 2010; *Isella et al.* 2009; *Guilloteau et al.* 2011). Even with these strong selection biases, the incidence of resolved cavities is surprisingly high compared to expectations from IR surveys (see § 4). *Andrews et al.* (2011b) estimated that at least 1 in 3 of these mm-bright (massive) disks exhibit large cavities.

Model fitting

The basic structures of disk cavities can be quantified through radiative transfer modeling of their SEDs (see § 2.1) simultaneously with resolved mm data. These models often assume that the cavity can be described as a region of sharply reduced dust surface densities (e.g., *Piétu et al.* 2006; *Brown et al.* 2008; *Hughes et al.* 2009; *Andrews et al.* 2011b; *Cieza et al.* 2012; *Mathews et al.* 2012). Such work finds cavity radii of $\sim$15–75 AU, depletion factors in the inner disk of $\sim 10^2$–10^5 relative to optically thick full disks, and outer regions with sizes and masses similar to those found for full disks. However, there are subtleties in this simple modeling prescription. First, the depletion levels are usually set by the infrared SED, not the mm data: the resolved images have a limited dynamic range and can only constrain an intensity drop by a factor $<$100. Second, and related, is that the "sharpness" of the cavity edge is unclear. The most popular model prescription implicitly imposes a discontinuity, but the data only directly indicate that the densities substantially decrease over a narrow radial range (a fraction of the still-coarse spatial resolution; $\sim$10 AU). Alternative models with a smoother taper at the cavity edge can explain the data equally well in many cases (e.g., *Isella et al.* 2010b, 2012; *Andrews et al.* 2011a), and might alleviate some of the tension with IR scattered light measurements (see § 2.3).

Some additional problematic issues with these simple models have been illuminated, thanks to a new focus on the details of the resolved mm data. For example, in some disks the dust ring morphology is found to be remarkably narrow – with nearly all of the emission coming from a belt 10-20 AU across (or less) – even as we trace gas with molecular line emission extending hundreds of AU beyond it (e.g., *Rosenfeld et al.* 2013). This hints at the presence of a particle "trap" near the cavity edge, as might be expected from local dynamical interactions between a planet and the gas disk (see § 3.2; *Zhu et al.* 2012; *Pinilla et al.* 2012). In a perhaps related phenomenon (e.g., *Regály et al.* 2012; *Birnstiel et al.* 2013), new high-fidelity images of (pre-)transitional disks are uncovering evidence that strong azimuthal asymmetries are common features of the mm emission rings (*Brown et al.* 2009; *Tang et al.* 2012; *Casassus et al.* 2013; *van der Marel et al.* 2013; *Isella et al.* 2013).

A number of pressing issues will soon be addressed by the ALMA project. Regarding the incidence of the disk holes and gaps, an expanded high resolution imaging census should determine the origin of the anomalously high occurrence of dust cavities in mm-wave images. If the detection rate estimated by *Andrews et al.* (2011b) is found to be valid at all luminosities, it would confirm that even the small amount of dust inside the disk cavities sometimes produces

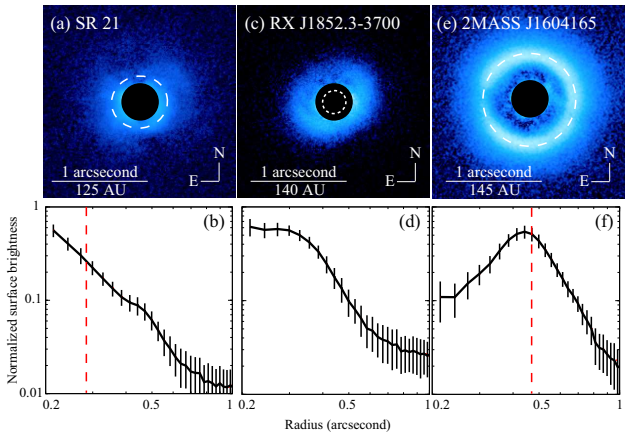

Fig. 5.— NIR polarimetric images of transitional disks in the H band (top; 1.6 μm) along with their averaged radial surface brightness profiles along the major disk axis (bottom). Broken lines in the top and bottom panels correspond to the radius of the outer wall as measured with submm imaging and/or SEDs. We note that the regions of the inner disk that cannot be resolved are masked out in the panels. From left to right the objects are as follows: SR 21 (*Follette et al.* 2013), RX J1852−3700 (*Kudo et al.*, in prep.), RX J1604−2130 (*Mayama et al.* 2012).

enough IR emission to hide the standard (pre-)transitional disk signature at short wavelengths, rendering IR selection inherently incomplete – something already hinted at in the current data. Perhaps more interesting would be evidence that the (pre-)transitional disk frequency depends on environmental factors, like disk mass (i.e., a selection bias) or stellar host properties (e.g., *Owen and Clarke* 2012). More detailed analyses of the disk structures are also necessary, both to develop a more appropriate modeling prescription and to better characterize the physical processes involved in clearing the disk cavities. Specific efforts toward resolving the depletion zone at the cavity boundary, searching for material in the inner disk, determining ring widths and measuring their mm/radio colors to infer the signatures of particle evolution and trapping (e.g., *Pinilla et al.* 2012; *Birnstiel et al.* 2013), and quantifying the ring substructures should all impart substantial benefits on our understanding of disks.

2.3 Infrared Imaging

IR imaging has been used successfully to observe disks around bright stars. Space-based observations free from atmospheric turbulence (e.g., HST) have detected fine disk structure such as spiral features in the disk of HD 100546 (*Grady et al.* 2001) and a ring-like gap in HD 141569 (*Weinberger et al.* 1999). MIR images of (pre-)transitional disks are able to trace the irradiated outer wall, which effectively emits thermal radiation (e.g., *Geers et al.* 2007; *Maaskant et al.* 2013). More recently, high-resolution NIR polarimetric imaging and IR interferometry has become available, allowing us to probe much further down into the inner few tens of AU in disks in nearby star-forming regions. Here we focus on NIR polarimetric and IR interferometric imaging of (pre-)transitional disks and also the results of IR imaging searches for companions in these objects.

NIR polarimetric imaging

NIR polarimetric imaging is capable of tracing the spatial distribution of submicron-sized dust grains located in the uppermost, surface layer of disks. One of the largest NIR polarimetry surveys of disks to date was conducted as part of the SEEDS (Strategic Explorations of Exoplanets and Disks with Subaru; *Tamura* 2009) project (e.g., Taurus at 140 pc; *Thalmann et al.* 2010; *Tanii et al.* 2012; *Hashimoto et al.* 2012; *Mayama et al.* 2012; *Follette et al.* 2013; *Takami et al.* 2013, *Tsukagoshi et al.*, submitted,). There is also VLT/NACO imaging work, predominantly focusing on disks around Herbig Ae/Be stars (*Quanz et al.* 2011, 2012, 2013a,b; *Rameau et al.* 2012). These surveys access the inner tens of AU in disks, reaching a spatial resolution of 0.06″ (8 AU) in nearby star-forming regions. Such observations have the potential to reveal fine structures such as spirals, warps, offsets, gaps, and dips in the disk.

Most of the (pre-)transitional disks around TTS observed by SEEDS have been resolved. This is because the stellar radiation can reach the outer disk more easily given that the innermost regions of (pre-)transitional disks are less dense than full disks. Many of these disks can be sorted into the three following categories based on their observed scattered light emission (i.e., their "polarized intensity" appearance) at 1.6 μm:

(A) No cavity in the NIR with a smooth radial surface brightness profile at the outer wall (e.g, SR 21; DoAr 44; RX J1615−3255; Fig. 5a, b),

(B) Similar to category A, but with a broken radial brightness profile (e.g. TW Hya; RX J1852.3−3700; LkHα 330). These disks display a slight slope in the radial brightness profile in the inner portion of the disk, but a steep slope in the outer regions (Fig. 5c, d),

(C) A clear cavity in the NIR polarized light (e.g., GM Aur; Sz 91; PDS 70; RX J1604-2130; Fig. 5e, f).

The above categories demonstrate that the spatial distribution of small and large dust grains in the disk are not necessarily similar. Based on previous submm images (see § 2.2), the large, mm-sized dust grains in the inner regions of each of the above disks is significantly depleted. However, in categories A and B there is evidence that a significant amount of small, submicron sized dust grains remains in the inner disk, well within the cavity seen in the submm images. In category C, the small dust grains appear to more closely trace the large dust distribution, as both are significantly depleted in the inner disk. One possible mechanism that could explain the differences between the three categories presented above is dust filtration (e.g., *Rice et al.* 2006; *Zhu et al.* 2012), which we will return to in more detail in § 3.2. More high-resolution imaging observations of disks at different wavelengths is necessary to develop a fuller picture of their structure given that the disk's appearance at a certain wavelength depends on the dust opacity.

IR interferometric imaging

IR interferometers, such as the Very Large Telescope Interferometer (VLTI), the Keck Interferometer (KI), and the CHARA array, provide milliarcsecond angular resolution in the NIR and MIR regime (1–13 μm), enabling new constraints on the structure of (pre-)transitional disks. Such spatially resolved studies are important to reveal complex structure in the small dust distribution within the innermost region of the disk, testing the basic constructs of models that have been derived based on spatially unresolved data (e.g., SEDs).

The visibility amplitudes measured with interferometry permit direct constraints on the brightness profile, and, through radiative transfer modeling (see § 2.1 and § 2.2 for discussion of limitations), on the distribution and physical conditions of the circumstellar material. The NIR emission (H and K band, $1.4 - 2.5\,\mu$m) in the pre-transitional disks studied most extensively with IR interferometry (i.e., HD 100546, T Cha, and V1247 Ori) is dominated by hot optically thick dust, with smaller contributions from scattered light (*Olofsson et al.* 2013) and optically thin dust emission (*Kraus et al.* 2013). The measured inner disk radii are in general consistent with the expected location of the dust sublimation radius, while the radial extent of this inner emission component varies significantly for different sources (HD 100546: 0.24–4 AU, *Benisty et al.* 2010; *Tatulli et al.* 2011; T Cha: 0.07–0.11 AU, *Olofsson et al.* 2011, 2013; V1247 Ori: 0.18–0.27 AU, *Kraus et al.* 2013).

The MIR regime (N band, $8 - 13\,\mu$m) is sensitive to a wider range of dust temperatures and stellocentric radii. In the transitional disk of TW Hya, the region inside of $0.3 - 0.52$ AU is found to contain only optically thin dust (*Eisner et al.* 2006; *Ratzka et al.* 2007; *Akeson et al.* 2011), followed by an optically thick outer disk (*Arnold et al.* 2012b), in agreement with SED modeling (*Calvet et al.* 2002) and (sub)mm imaging (*Hughes et al.* 2007). The gaps in the pre-transitional disks of the Herbig Ae/Be star HD 100546 (*Mulders et al.* 2013) and the TTS T Cha (*Olofsson et al.* 2011, 2013) were found to be highly depleted of (sub)μm-sized dust grains, with no significant NIR or MIR emission, consistent with SED-based expectations (i.e., no substantial 10 μm silicate emission). The disk around the Herbig Ae/Be star V1247 Ori, on the other hand, exhibits a gap filled with optically thin dust. The presence of such optically thin material within the gap is not evident from the SED, while the interferometric observations indicate that this gap material is the dominant contributor at MIR wavelengths. This illustrates the importance of IR interferometry for unraveling the physical conditions in disk gaps and holes.

We note that besides the dust continuum emission, some (pre-)transitional disks exhibit polycyclic aromatic hydrocarbon (PAH) spectral features, for instance at 7.7 μm, 8.6 μm, and 11.3 μm. For a few objects, it was possible to locate the spatial origin of these features using adaptive optics imaging (*Habart et al.* 2006) or MIDI long-baseline interferometry (*Kraus* 2013). These observations showed that these molecular bands originate from a significantly more extended region than the NIR/MIR continuum emission, including the gap region and the outer disk. This is consistent with the scenario that these particles are transiently heated by UV photons and can be observed over a wide range of stellocentric radii.

One of the most intriguing findings obtained with IR interferometry is the detection of non-zero phase signals, which indicate the presence of significant asymmetries in the inner, AU-scale disk regions. Keck/NIRC2 aperture masking observations of V1247 Ori (*Kraus et al.* 2013) revealed asymmetries whose direction is not aligned with the disk minor axis and also changes with wavelength. Therefore, these asymmetries are neither consistent with a companion detection, nor with disk features. Instead, these observations suggest the presence of complex, radially extended disk structures, located within the gap region. It is possible that these structures are related to the spiral-like inhomogeneities that have been detected with coronagraphic imaging on about 10-times larger scales (e.g., *Hashimoto et al.* 2011; *Grady et al.* 2013) and that they reflect the dynamical interaction of the gap-opening body/bodies with the disk material. Studying these complex density structures and relating the asymmetries to the known spectrophotometric variability of these objects (§ 2.4) will be a major objective of future interferometric imaging studies.

The major limitations from the existing studies arise from sparse uv-coverage, which has so far prevented the reconstruction of direct interferometric images for these objects. Different strategies have been employed in order to relax the uv-coverage restrictions, including the combination of long-baseline interferometric data with single-aperture interferometry techniques (e.g., speckle and aperture masking interferometry; *Arnold et al.* 2012b; *Olofsson et al.* 2013; *Kraus et al.* 2013) and the combination of data from different facilities (*Akeson et al.* 2011; *Olofsson et al.* 2013; *Kraus et al.* 2013). Truly transformational results can be expected from the upcoming generation of imaging-optimized long-baseline interferometric instruments, such as the 4-telescope MIR beam combiner MATISSE, which will enable efficient long-baseline interferometric imaging on scales of several AU.

Companion Detections

NIR imaging observations can directly reveal companions within the cleared regions of disks. Both theory and observations have long shown that stellar binary companions can open gaps (e.g., *Artymowicz and Lubow* 1994; *Jensen and Mathieu* 1997; *White and Ghez* 2001), based on numerous moderate-contrast companions ($\sim$0–3 magnitudes of contrast, or companion masses $> 0.1 M_{\odot}$) that have been identified with RV monitoring, HST imaging, adaptive optics imaging, and speckle interferometry. For example, NIR imaging of CoKu Tau/4, a star surrounded by a transitional disk, revealed a previously unknown stellar-mass companion that is likely responsible for the inner clearing

in this disk, demonstrating that it is very important to survey stars with (pre-)transitional disks for binarity in addition to exploring other possible clearing mechanisms (see § 3.2; *Ireland and Kraus* 2008).

The detection of substellar or planetary companions has been more challenging, due to the need for high contrast ($\Delta L'$ =5 to achieve $M_{lim} = 30 M_{Jup}$ for a 1 $M_{\odot}$ primary star) near or inside the formal diffraction limit of large telescopes. Most of the high-contrast candidate companions identified to date have been observed with interferometric techniques such as nonredundant mask interferometry (NRM; *Tuthill et al.* 2000; *Ireland* 2012), which measure more stable observable quantities (such as closure phase) to achieve limits of $\Delta L'$ =7–8 at λ/D (3–5 M_{Jup} at 8 AU). The discoveries of NRM include a candidate planetary-mass companion to LkCa 15 (*Kraus and Ireland* 2012) and a candidate low-mass stellar companion to T Cha (*Huélamo et al.* 2011). A possible candidate companion was reported around FL Cha, although these asymmetries could be associated with disk emission instead (*Cieza et al.* 2013).

Advanced imaging techniques also are beginning to reveal candidate companions at intermediate orbital radii that correspond to the optically thick outer regions of (pre-)transitional disks (e.g., *Quanz et al.* 2013a), beyond the outer edge of the hole or gap region. The flux contributions of companions can be difficult to distinguish from scattered light due to disk features (*Olofsson et al.* 2013; *Cieza et al.* 2013; *Kraus et al.* 2013). However, the case of LkCa 15 shows that the planetary hypothesis can be tested using multi-epoch, multi-wavelength data (to confirm colors and Keplerian orbital motion) and by direct comparison to resolved submm maps (to localize the candidate companion with respect to the inner disk edge).

Even with the enhanced resolution and contrast of techniques like NRM, current surveys are only able to probe super-Jupiter masses in outer solar systems. For bright stars ($I \lesssim 9$), upcoming extreme adaptive optics systems like GPI and SPHERE will pave the way to higher contrasts with both imaging and NRM, achieving contrasts of $\Delta K \geq 10$ at λ/D ($\sim$1–2 M_{Jup} at 10 AU). However, most young solar-type and low-mass stars fall below the optical flux limits of extreme AO. Further advances for those targets will require observations with JWST that probe the sub-Jupiter regime for outer solar systems (ΔM $\sim$10 at λ/D, or $<$1 M_{Jup} at $>$15 AU) or with future ground-based telescopes that probe the Jupiter regime near the snow line (achieving ΔK $\sim$10 at λ/D or $\sim$1–2 M_{Jup} at $>$2–3 AU).

2.4 Time domain studies

IR variability in TTS is ubiquitous and several ground-based studies have been undertaken to ascertain the nature of this variability (e.g., *Joy* 1945; *Rydgren et al.* 1976; *Carpenter et al.* 2001). With the simultaneous MIR wavelength coverage provided by *Spitzer* IRS, striking variability in (pre)-transitional disks was discovered, suggestive of structural changes in these disks with time. We review this variability along with the mechanisms that have been proposed to be responsible for it in the following subsections.

"Seesaw" variability

The flux in many pre-transitional disks observed for variability to date "seesaws," i.e., as the emission decreases at shorter wavelengths in the IRS data, the emission increases at longer wavelengths (Fig. 6; *Muzerolle et al.* 2009; *Espaillat et al.* 2011; *Flaherty et al.* 2012). MIR variability with IRS was also seen in some transitional disks (e.g., GM Aur and LRLL 67; *Espaillat et al.* 2011; *Flaherty et al.* 2012), though in these objects the variability was predominantly around the region of the silicate emission feature. Typically, the flux in the pre-transitional disks and transitional disks observed changed by about 10% between epochs, but in some objects the change was as high as 50%.

This variability may point to structural changes in disks. SED modeling can explain the seesaw behavior seen in pre-transitional disks by changing the height of the inner wall of these disks (Fig. 7; *Espaillat et al.* 2011). When the inner wall is taller, the emission at the shorter wavelengths is higher since the inner wall dominates the emission at 2-8 μm. The taller inner wall casts a larger shadow on the outer disk wall, leading to less emission at wavelengths beyond 20 μm where the outer wall dominates. When the inner wall is shorter, the emission at the shorter wavelengths is lower and the shorter inner wall casts a smaller shadow on the outer disk wall, leading to more emission at longer wavelengths. This "seesaw" variability confirms the presence of optically thick material in the inner disk of pre-transitional disks. The variability seen in transitional disks may suggest that while the disk is vertically optically thin, there is a radially optically thick structure in the inner disk, perhaps composed of large grains and/or limited in spatial extent so that it does not contribute substantially to the emission between 1–5 μm while still leading to shadowing of the outer disk. One intriguing possibility involves accretion streams connecting multiple planets, as predicted in the models of *Zhu et al.* (2011); *Dodson-Robinson and Salyk* (2011) and claimed to be seen by ALMA (*Casassus et al.* 2013).

Possible underlying mechanisms

When comparing the nature of the observed variability to currently known physical mechanisms, it seems unlikely that star spots, winds, and stellar magnetic fields are the underlying cause. The star spots proposed to explain variability at shorter wavelengths in other works (e.g., *Carpenter et al.* 2001) could change the irradiation heating, but this would cause an overall increase or decrease of the flux, not seesaw variability. A disk wind which carries dust may shadow the outer disk. However, *Flaherty et al.* (2011) do not find evidence for strong winds in their sample which displays seesaw variability. Stellar magnetic fields that interact with dust beyond the dust sublimation radius may lead to changes if the field expands and contracts or is tilted

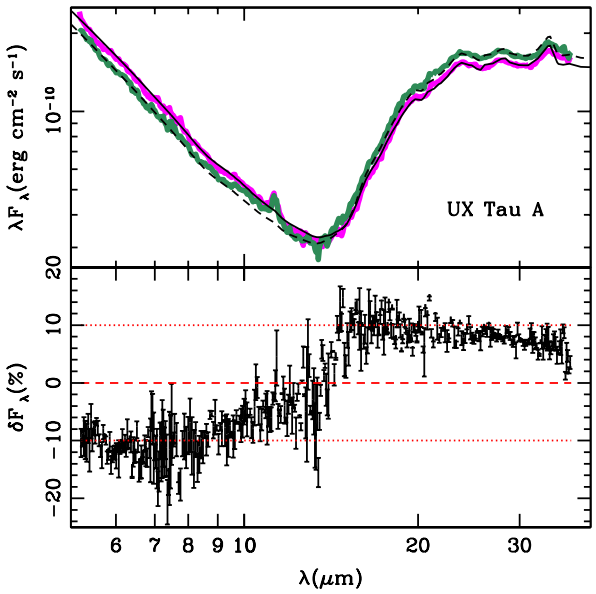

Fig. 6.— Top: Observed *Spitzer* IRS spectra (gray) and models (solid and broken black lines) for the pre-transitional disk of UX Tau A. The variability between the two spectra can be reproduced by changing the height of the inner disk wall in the model by 17%. Bottom: Percentage change in flux between the two IRS spectra above. The observed variability cannot be explained by the observational uncertainties of IRS (error bars). Figure adapted from *Espaillat et al.* (2011).

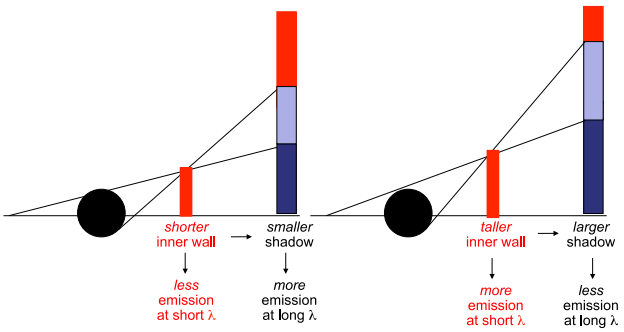

Fig. 7.— Schematic depicting the proposed link between the observed variability and disk structure based on the SED modeling from Fig. 6. Medium gray corresponds to visible areas of the disk wall, while light gray and dark gray areas are in the penumbra and umbra, respectively. The MIR variability observed in pre-transitional disks can be explained by changes in the height of the inner disk wall, which results in variable shadowing of the outer wall.

with respect to plane of the disk (*Goodson and Winglee* 1999; *Lai and Zhang* 2008). However, it is thought that the stellar magnetic field truncates the disk within the corotation radius and for many objects. The corotation radius is within the dust sublimation radius, making it unlikely that the stellar magnetic field is interacting with the dust in the disk (*Flaherty et al.* 2011).

It is unclear what role accretion or X-ray flares may play in disk variability. Accretion rates are known to be variable in young objects, but *Flaherty et al.* (2012) do not find that the observed variations in accretion rate are large enough to reproduce the magnitude of the MIR variability observed. Strong X-ray flares can increase the ionization of dust and lead to a change in scale height (*Ke et al.* 2012). However, while TTS are known to have strong X-ray flares (*Feigelson et al.* 2007), it is unlikely that all of the MIR disk variability observed overlapped with strong X-ray flares.

The MIR variability seen is most likely due to perturbations in the disk, possibly by planets or turbulence. Planets are thought to create spiral density waves in the disk (see PPV review by *Durisen et al.* 2007), which may have already been detected in disks (e.g., *Hashimoto et al.* 2011; *Grady et al.* 2013). Such spiral density waves may affect the innermost disk, causing the height of the inner disk wall to change with time and creating the seesaw variability observed. The timescales of the variability discussed here span ∼1–3 years down to 1 week or less. If the variability is related to an orbital timescale, this corresponds to ∼1–2 AU and <0.07 AU in the disk, plausible locations for planetary companions given our own solar system and detections of hot Jupiters (*Marcy et al.* 2005). Turbulence is also a viable solution. Magnetic fields in a turbulent disk may lift dust and gas off the disk (*Turner et al.* 2010; *Hirose and Turner* 2011). The predicted magnitude of such changes in the disk scale height are consistent with the observations.

Observations with *JWST* can explore the range of timescales and variability present in (pre-)transitional disks to test all of the scenarios explored above. It is also likely that a diverse range of variability is present in most disks around young stars (e.g., YSOVAR; *Morales-Calderón et al.* 2011) and *JWST* observations of a wide range of disks will help us more fully categorize disk variability.

2.5 Gaseous Emission

The structure of the gas in (pre-)transitional disks is a valuable probe, because the mechanisms proposed to account for the properties of these objects (§ 3; e.g., grain growth, photoevaporation, companions) may impact the gas in different ways from the dust. The chapters in this volume by *Pontoppidan et al.* and *Alexander et al.* as well as the earlier PPV review by *Najita et al.* (2007b), describe some of the available atomic and molecular diagnostics and how they are used to study gas disks. In selecting among these specifically for the purpose of probing radial disk structure, it is important to consider how much gas is expected to remain in a hole or gap. Although theoretical studies suggest the gas column density is significantly reduced in the cleared dust region (e.g., by ∼ 1000; *Regály et al.* 2010),

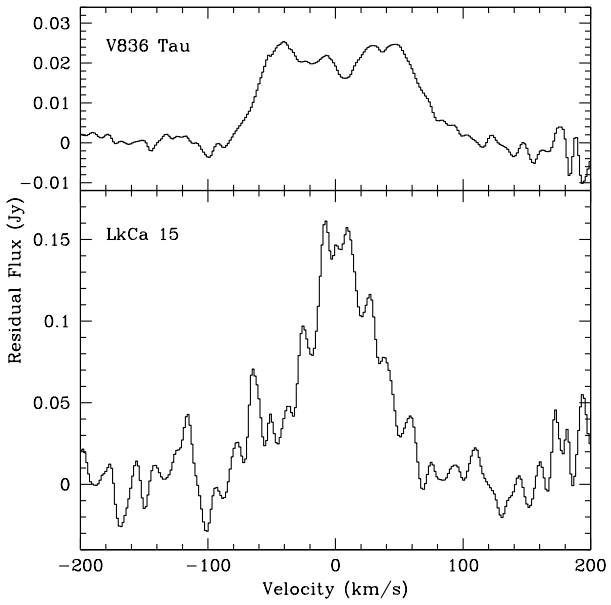

Fig. 8.— Rovibrational line profiles of CO v=1–0 emission from V836 Tau (top) and LkCa 15 (bottom) after correction for stellar CO absorption (*Najita et al.* 2008). The double-peaked profile of V836 Tau indicates that the gas emission is truncated beyond ~ 0.4 AU. The centrally-peaked LkCa 15 profile indicates gas emission extending to much larger radii.

given a typical TTS's disk column density of 100 g/cm^2 at 1 AU, a fairly hefty gas column density could remain. Many stars hosting (pre-)transitional disks also show signs of significant gas accretion (§ 4.2). These considerations suggest that molecular diagnostics, which probe larger disk column densities ($N_H > 1\times10^{21}$ cm^{-2}), are more likely to be successful in detecting a hole or gap in the gas disk. In the following, we review what is known to date about the radial structure of gas in disks.

MIR and (sub)mm spectral lines

As there are now gas diagnostics that probe disks over a wide range of radii ($\sim 0.1 - 100$ AU), the presence or absence of these diagnostics in emission can give a rough idea of whether gas disks are radially continuous or not. At large radii, the outer disks of many (pre-)transitional disks (TW Hya, GM Aur, DM Tau, LkCa 15, etc.) are well studied at mm wavelengths (e.g., *Koerner and Sargent* 1995; *Guilloteau and Dutrey* 1994; *Dutrey et al.* 2008, see also § 2.2). For some, the mm observations indicate that rotationally excited CO exists within the cavity in the dust distribution (e.g., TW Hya, LkCa 15; *Rosenfeld et al.* 2012; *Piétu et al.* 2007), although these observations cannot currently constrain how that gas is distributed. Many (pre-)transitional disks also show multiple signatures of gas close to the star: ongoing accretion (§ 4.2), UV H_2 emission (e.g., *Ingleby et al.* 2009; *France et al.* 2012), and rovibrational CO emission (*Salyk et al.* 2009, 2011; *Najita et al.* 2008, 2009).

In contrast, the 10-20 μm *Spitzer* spectra of these objects conspicuously lack the rich molecular emission (e.g., H_2O, C_2H_2, HCN) that characterizes the mid-infrared spectra of full disks around classical TTS (CTTS, i.e., stars that are accreting; *Najita et al.* 2010; *Pontoppidan et al.* 2010). As these MIR molecular diagnostics probe radii within a few AU of the star, their absence is suggestive of a missing molecular disk at these radii, i.e., a gap between an inner disk (traced by CO and UV H_2) and the outer disk (probed in the mm). Alternatively, the disk might be too cool to emit at these radii, or the gas may be abundant but in atomic form. Further work, theoretical and/or observational, is needed to evaluate these possibilities.

Velocity resolved spectroscopy

Several approaches can be used to probe the distribution of the gas in greater detail. In the absence of spatially resolved imaging, which is the most robust approach, velocity resolved spectroscopy coupled with the assumption of Keplerian rotation can probe the radial structure of gaseous disks (see PPIV review by *Najita et al.* 2000). The addition of spectroastrometric information (i.e., the spatial centroid of spectrally resolved line emission as a function of velocity) can reduce ambiguities in the disk properties inferred with this approach (*Pontoppidan et al.* 2008). These techniques have been used to search for sharp changes in gaseous emission as a function of radius as evidence of disk cavities, and to identify departures from azimuthal symmetry such as those created by orbiting companions.

Velocity resolved spectroscopy of CO rovibrational emission provides tentative evidence for a truncated inner gas disk in the evolved disk V836 Tau (*Strom et al.* 1989). An optically thin gap, if there is one, would be found at small radii ($\sim$ 1 AU) and plausibly overlap the range of disk radii probed by the CO emission. Indeed, the CO emission from V836 Tau is unusual in showing a distinct double-peaked profile consistent with the truncation of the CO emission beyond ~ 0.4 AU (Fig. 8; *Najita et al.* 2008). In comparison, other disks show much more centrally peaked rovibrational CO line profiles (*Salyk et al.* 2007, 2009; *Najita et al.* 2008, 2009).

Spectroscopy also indicates possible differences in the radial extent of the gas and dust in the inner disk. The CO emission profile from the pre-transitional disk of LkCa 15 (Fig. 8; *Najita et al.* 2008) spans a broad range of velocities, indicating that the inner gas disk extends over a much larger range of radii (from ~ 0.08 AU out to several AU) than in V836 Tau. This result might be surprising given that SED modeling suggests that the inner optically thick dust disk of LkCa 15 extends over a narrow annular region (0.15–0.19 AU; *Espaillat et al.* 2010). The origin of possible differences in the radial extent of the gas and dust in the inner disk region is an interesting topic for future work.

Some of the best evidence to date for the truncation of the outer gas disks of (pre-)transitional disks comes from studies of Herbig Ae/Be stars. For nearby systems with large dust cavities, ground-based observations can spatially resolve the inner edge of the CO rovibrational emis-

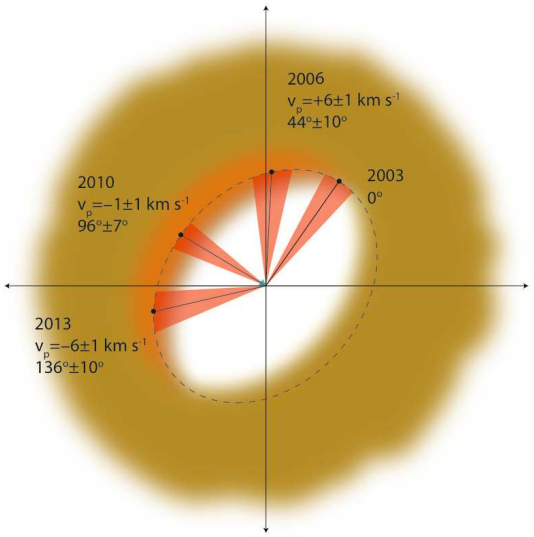

Fig. 9.— Spectroastrometry of the CO rovibrational emission from HD100546, followed over 10 years, reveals evidence for a compact source of CO emission that orbits the star near the inner disk edge (*Brittain et al.* 2013, and 2014, in preparation). Possible interpretations include emission from a circumplanetary disk or a hot spot heated by an orbiting companion.

sion from the outer disks around these bright stars (e.g., HD141569; *Goto et al.* 2006). Line profile shapes and constraints from UV fluorescence modeling have also been used to show that rovibrational CO and OH emission is truncated at the same radius as the disk continuum in some systems (*Brittain et al.* 2007; *van der Plas et al.* 2009; *Brittain et al.* 2009; *Liskowsky et al.* 2012), although the radial distribution of the gas and dust appear to differ in other systems (e.g., IRS 48; *Brown et al.* 2012). The gas disk may sometimes be truncated significantly inward of the outer dust disk and far from the star. For example, the CO emission from SR 21 extends much further in (to ∼7 AU) than the inner hole size of ∼18 AU (*Pontoppidan et al.* 2008).

Several unusual aspects of the gaseous emission from HD100546 point to the possibility that the cavity in the molecular emission is created by an orbiting high mass giant planet. *Acke and van den Ancker* (2006) inferred the presence of a gap in the gas disk based on a local minimum in the [O I] 6300 Å emission from the disk. The rovibrational OH emission from HD100546 is found to show a strong line asymmetry that is consistent with emission from an eccentric inner rim ($e \geq 0.18$; *Liskowsky et al.* 2012). Eccentricities of that magnitude are predicted to result from planet-disk interactions (e.g., *Papaloizou et al.* 2001; *Kley and Dirksen* 2006). In addition, the CO rovibrational emission varies in its spectroastrometric signal. The variations can be explained by a CO emission component that orbits the star just within the 13 AU inner rim (Fig. 9; *Brittain et al.* 2013). The required emitting area (0.1 AU^2) is similar to that expected for a circumplanetary disk surrounding a $5M_J$ planet at that distance (e.g., *Quillen and Trilling* 1998; *Martin and Lubow* 2011). Further studies with ALMA and ELTs will give us new opportunities to explore the nature of disk holes and gaps in the gas disk (e.g., *van der Marel et al.* 2013; *Casassus et al.* 2013).

3. COMPARISON TO THEORETICAL MECHANISMS

There are three main observational constraints every theory must confront when attempting to explain (pre-)transitional disk observations. First, the cleared regions in (pre-)transitional disks studied to date are generally large (§ 2.1, § 2.2). For transitional disks, the optically thin region extends from tens of AU all the way down to the central star. For pre-transitional disks, SED modeling suggests that the optically thick region may only extend up to ∼ 1 AU, followed by a gap that is significantly depleted of dust up to tens of AU, as seen in the transitional disks. At the same time, submm imaging has revealed the existence of some disks which have inner regions significantly depleted of large dust grains without exhibiting MIR SED deficits (§ 2.2), suggesting that a large amount of small dust grains still remain in the inner disk, as also shown by NIR polarimetric images (§ 2.3). Second, in order to be discernible in the SED, the gaps/holes need to be optically thin which implies that the mass of small dust grains (of order a micron or less) must be extremely low. Third, while most (pre-)transitional disks accrete onto the central star at a rate which is lower than the median accretion rate for TTS (∼$10^{-8} M_\odot\, yr^{-1}$; *Hartmann et al.* 1998, § 4.2), their rates are still substantial (§ 4.2). This indicates that considerable gas is located within the inner disk, although we currently do not have many constraints on how this gas is spatially distributed. In the following sections, we review the clearing mechanisms that have been applied to explain (pre-)transitional disk observations in light of the above constraints.

3.1 Non-dynamical Clearing Mechanisms

A diverse set of physical mechanisms has been invoked to explain (pre-)transitional disk observations, with varying levels of success. Much of the attention is focused on dynamical interactions with one or more companion objects, although that subject will be addressed separately in § 3.2. There are a number of alternative scenarios that merit review here, including the effects of viscous evolution, particle growth and migration, and dispersal by (photoevaporative) winds.

Viscous evolution

The interactions of gravitational and viscous torques comprise the dominant mechanism for the structural evolution of disks over most of their lifetimes (*Lynden-Bell and Pringle* 1974; *Hartmann et al.* 1998). An anomalous kinematic viscosity, presumably generated by MHD turbulence,

drives a persistent inward flow of gas toward the central star (e.g., *Hartmann et al.* 2006). Angular momentum is transported outward in that process, resulting in some disk material being simultaneously spread out to large radii. As time progresses, the disk mass and accretion rate steadily decline. To first order, this evolution is self-similar, so there is no preferential scale for the depletion of disk material. The nominal viscous evolution ($\sim$depletion) timescales at 10s of AU are long, comparable to the stellar host ages.

If the gas and dust were perfectly coupled, we would expect viscous evolution acting alone to first produce a slight enhancement in the FIR/mm SED (due to the spreading of material out to larger radii) and then settle into a slow, steady dimming across the SED (as densities decay). Coupled with the sedimentation of disk solids, these effects are a reasonable explanation for the evolved disks (§ 2.1). That said, there is no reason to expect that viscous effects alone are capable of the preferential depletion of dust at small radii needed to produce the large cleared regions typical of (pre-)transitional disks. Even in the case of enhanced viscosity in the outer wall due to the magneto-rotational instability (MRI *Chiang and Murray-Clay* 2007), this needs a pre-existing inner hole to have been formed via another mechanism in order to be effective.

Grain growth

The natural evolution of dust in a gas-rich environment offers two complementary avenues for producing the observable signatures of holes and gaps in disks. First is the actual removal of material due to the inward migration and subsequent accretion of dust particles. This "radial drift" occurs because thermal pressure causes the gas to orbit at subKeplerian rates, creating a drag force on the particles that saps their orbital energy and sends them spiraling in to the central star (*Whipple* 1972; *Weidenschilling* 1977; *Brauer et al.* 2008). Swept up in this particle flow, the reservoir of emitting grains in the inner disk can be sufficiently depleted to produce a telltale dip in the IR SED (e.g., *Birnstiel et al.* 2012). A second process is related to the actual growth of dust grains. Instead of a decrease in the dust densities, the inner disk only appears to be cleared due to a decrease in the grain emissivities: larger particles emit less efficiently (e.g., *D'Alessio et al.* 2001; *Draine* 2006). Because growth timescales are short in the inner disk, the IR emission that traces those regions could be suppressed enough to again produce a dip in the SED.

The initial models of grain growth predicted a substantial reduction of small grains in the inner disk on short timescales, and therefore a disk clearing signature in the IR SED (*Dullemond and Dominik* 2005; *Tanaka et al.* 2005). More detailed models bear out those early predictions, even when processes that decrease the efficiency (e.g., fragmentation) are taken into account. *Birnstiel et al.* (2012) demonstrated that such models can account for the IR SED deficit of transitional disks by tuning the local conditions so that small ($\sim\mu$m-sized) particles in the inner disk grow efficiently to mm/cm sizes. However, those particles cannot grow much larger before their collisions become destructive: the resulting population of fragments would then produce sufficient emission to wash out the infrared SED dip. The fundamental problem is that those large particles emit efficiently at mm/cm wavelengths, so these models do not simultaneously account for the ring-like emission morphologies observed with interferometers (Fig. 4). *Birnstiel et al.* (2012) argued that the dilemma of this conflicting relationship between growth/fragmentation and the IR/mm emission diagnostics means that particle evolution *alone* is not the underlying cause of cavities in disks.

A more in-depth discussion of these and other issues related to the observational signatures of grain growth and migration are addressed in the chapter by *Testi et al.* in this volume.

Photoevaporation

Another mechanism for sculpting (pre-)transitional disk structures relies on the complementary interactions of viscous evolution, dust migration, and disk dispersal via photoevaporative winds (*Hollenbach et al.* 1994; *Clarke et al.* 2001; *Alexander et al.* 2006; *Alexander and Armitage* 2007; *Gorti and Hollenbach* 2009; *Gorti et al.* 2009; *Owen et al.* 2010, 2011; *Rosotti et al.* 2013). Here, the basic idea is that the high-energy irradiation of the disk surface by the central star can drive mass-loss in a wind that will eventually limit the re-supply of inner disk material from accretion flows. Once that occurs, the inner disk can rapidly accrete onto the star, leaving behind a large (and potentially growing) hole at the disk center. The detailed physics of this process can be quite complicated, and depend intimately on how the disk is irradiated. The chapter in this volume by *Alexander et al.* provides a more nuanced perspective on this process, as well as on the key observational features that support its presumably important role in disk evolution in general, and the (pre-)transitional disk phenomenon in particular.

However, for the subsample of (pre-)transitional disks that have been studied in detail, the combination of large sizes and tenuous (but non-negligible) contents of the inner disks (§ 2.1, 2.2, 2.3), substantial accretion rates (§ 4.2), and relatively low X-ray luminosities (§ 4.3) indicate that photoevaporation does not seem to be a viable mechanism for the depletion of their inner disks (e.g., *Alexander and Armitage* 2009; *Owen et al.* 2011; *Bae et al.* 2013a). In addition, there exist disks with very low accretion rates onto the star that do not show evidence of holes or gaps in the inner disk (*Ingleby et al.* 2012).

3.2 Dynamical Clearing by Companions

Much of the theoretical work conducted to explain the clearings seen in disks has focused on dynamical interactions with companions. When a second gravitational source is present in the disk, it can open a gap (*Papaloizou et al.* 2007; *Crida et al.* 2006; *Kley and Nelson* 2012, see chapter by *Baruteau et al.* in this volume). The salient issue is whether this companion is a star or a planet. It has been

shown both theoretically and observationally that a stellar-mass companion can open a gap in a disk. For example, CoKu Tau/4 is surrounded by a transitional disk (*D'Alessio et al.* 2005) and it has a nearly equal mass companion with a separation of 8 AU (§ 2.3; *Ireland and Kraus* 2008). Such a binary system is expected to open a cavity at 16–24 AU (*Artymowicz and Lubow* 1994), which is consistent with the observations (*D'Alessio et al.* 2005; *Nagel et al.* 2010). Here we focus our efforts on discussing dynamical clearing by planets. A confirmed detection of a planet in a disk around a young star does not yet exist. Therefore, it is less clear if dynamical clearing by planets is at work in some or most (pre-)transitional disks. Given the challenges in detecting young planets in disks, the best we can do at present is theoretically explore what observational signatures would be present if there were indeed planets in disks and to test if this is consistent with what has been observed to date, as we will do in the following subsections.

Maintaining gas accretion across holes and gaps

A serious challenge for almost all theoretical disk clearing models posed to date is the fact that some (pre-)transitional disks exhibit large dust clearings while still maintaining significant gas accretion rates onto the star. Compared to other disk clearing mechanisms (see § 3.1), gap opening by planets can more easily maintain gas accretion across the gap since the gravitational force of a planet can "pull" the gas from the outer disk into the inner disk.

The gap's depth and the gas accretion rate across the gap are closely related. The disk accretion rate at any radius R is defined as $\dot{M} = 2\pi R\langle\Sigma v_r\rangle$, where Σ and v_r are the gas surface density and radial velocity at R. If we further assume $\langle\Sigma v_r\rangle$=$\langle\Sigma\rangle\langle v_r\rangle$ and the accretion rate across the gap is a constant, the flow velocity is accelerated by about a factor of 100 in a gap which is a factor of 100 in depth.

In a slightly more realistic picture, $\langle\Sigma v_R\rangle$=$\langle\Sigma\rangle\langle v_R\rangle$ breaks down within the gap since the planet-disk interaction is highly asymmetric in the R-ϕ 2-D plane. Inside of the gap, the flow only moves radially at the turnover of the horseshoe orbit, which is very close to the planet. This high velocity flow can interact with the circumplanetary material, shock with and accrete onto the circumplanetary disk, and eventually onto the protoplanet (*Lubow et al.* 1999). Due to the great complexity of this process, the ratio between the accretion onto the planet and the disk's accretion rate across the gap is unclear. Thus, we will parameterize this accretion efficiency onto the planet as ξ. After passing the planet, the accretion rate onto the star is only $1-\xi$ of the accretion rate of the case where no planet is present. Note that this parameterization assumes that the planet mass is larger than the local disk mass so that the planet migration is slower than the typical type II rate. For a disk with $\alpha = 0.01$ and $\sim 10^{-8} M_\odot\, yr^{-1}$, the local disk mass is 1.5 M_J at 20 AU. *Lubow and D'Angelo* (2006) carried out 3-D viscous hydrodynamic simulations with a sink particle as the planet and found a ξ of 0.9. *Zhu et al.* (2011) carried out 2-D viscous hydro-simulations, but depleted the circumplanetary material at different timescales, and found that ξ can range between 0.1-0.9 depending on the circumplanetary disk accretion timescale. The accretion efficiency onto the planet plays an essential role in the accretion rate onto the star.

Explaining IR SED deficits

Regardless of the accretion efficiency, there is an intrinsic tension between significant gas accretion rates onto the star and the optically thin inner disk region in (pre-)transitional disks. This is because the planet's influence on the accretion flow of the disk is limited to the gap region (*Crida et al.* 2006) whose outer and inner edge hardly differ by a factor of more than 2. After passing through the gap, the inner disk surface density is again controlled only by the accretion rate and viscosity (e.g., MHD turbulence), similar to a full disk. Since a full disk's inner disk produces strong NIR emission, it follows that transitional disks should also produce strong NIR emission, but they do not.

With this simple picture it is very difficult to explain transitional disks, which have strong NIR deficits, compared to pre-transitional disks. For example, the transitional disk GM Aur has very weak NIR emission. It has an optically thin inner disk at 10 μm with an optical depth of $\sim$0.01 and an accretion rate of $\sim 10^{-8} M_\odot\, yr^{-1}$. Using a viscous disk model with $\alpha = 0.01$, Σ_g is derived to be 10–100 g/cm^2 at 0.1 AU. Considering that the nominal opacity of ISM dust at 10 μm is 10 cm^2/g, the optical depth at 10 μm for the inner disk is 100–1000 (*Zhu et al.* 2011), which is 4–5 orders of magnitude larger than the optical depth (~ 0.01) derived from observations.

In order to resolve the conflict between maintaining gas accretion across large holes and gaps while explaining weak NIR emission, several approaches are possible. In the following sections, we will outline two of these, namely multiple giant planets and dust filtration along with their observational signatures.

A possible solution: multiple giant planets

One possibility is that multiple planets are present in (pre-)transitional disks. If multiple planets from 0.1 AU to tens of AU can open a mutual gap, the gas flow can be continuously accelerated and passes from one planet to another so that a low disk surface density can sustain a substantial disk accretion rate onto the star (*Zhu et al.* 2011; *Dodson-Robinson and Salyk* 2011). However, hydrodynamical simulations have shown that each planet pair in a multiple planet system will move into 2:1 mean motion resonance (*Pierens and Nelson* 2008). Even in a case with four giant planets, with the outermost one located at 20 AU, the mutual gap is from 2-20 AU (*Zhu et al.* 2011). Therefore, to affect the gas flow at 0.1 AU, we need to invoke an even higher number of giant planets.

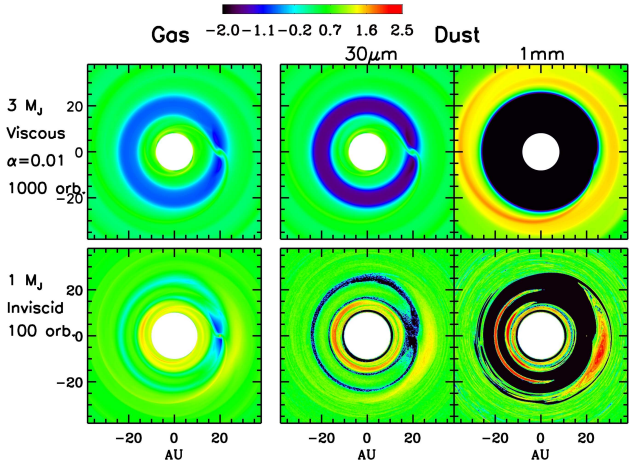

Fig. 10.— The disk surface density for the gas (left) and dust (right) in viscous (α=0.01, top) and inviscid (bottom) simulations. In the viscously accreting disk, the accretion flow carries small particles from the outer disk to the inner disk while big particles are deposited at the gap edge. In the inviscid disk, particles are trapped in the vortex at the gap edge and the planet co-orbital region. Figure adapted from *Zhu et al.* (2012) and *Zhu et al.*, in press.

If there are multiple planets present in (pre-)transitional disks, the planet accretion efficiency parameter (ξ) cannot be large in order to maintain a moderate accretion rate onto the star. With N planets in the disk, the accretion rate onto the star will be $(1-\xi)^N \dot{M}_{full}$. If $\xi = 0.9$ and the full disk has a nominal accretion rate $\dot{M}_{full} = 10^{-8} M_\odot\, yr^{-1}$, after passing two planets the accretion rate is $0.01\times\ 10^{-8} M_\odot\, yr^{-1}$=$10^{-10} M_\odot\, yr^{-1}$ which is already below the observed accretion rates in (pre-)transitional disks (see § 4.2). On the other hand, if $\xi = 0.1$, even with four planets, the disk can still accrete at $(1-0.1)^4 \dot{M}_{full} = 0.66 \dot{M}_{full}$. Thus, ξ is one key parameter in the multi-planet scenario, which demands further study.

Another possible solution: dust filtration

Another possibility is that the small dust grains in the inner disk are highly depleted by physical removal or grain growth, to the point where the dust opacity in the NIR is far smaller than the ISM opacity. Generally, this dust opacity depletion factor is $\sim 10^3$ to 10^5 (*Zhu et al.* 2011). Dust filtration is a promising mechanism to deplete dust to such a degree.

Dust filtration relies on the fact that dust and gas in disks are not perfectly coupled. Due to gas drag, dust particles will drift towards a pressure maximum in a disk (see chapter by *Johansen et al.* in this volume; *Weidenschilling* 1977). The drift speed depends on the particle size, and particles with the dimensionless stopping time $T_s = t_s \Omega \sim 1$ drift fastest in disks. If the particle is in the Epstein regime (when a particle is smaller than molecule mean-free-path) and has a density of 1 $\mathrm{g\,cm^{-3}}$, T_s is related to the particle size, s, and the disk surface density, Σ_g, as $T_s = 1.55 \times 10^{-3} (s/1\,\mathrm{mm})(100\,\mathrm{g\,cm^{-2}}/\Sigma_g)$ (*Weidenschilling* 1977). In the outer part of the disk (e.g., ∼50 AU) where $\Sigma_g \sim 1$ or 10 g $\mathrm{cm^{-2}}$, 1 cm particles have $T_s \sim 1$ or 0.1. Thus, submm and cm observations are ideal to reveal the effects of particle drift in disks. At the outer edge of a planet-induced gap, where the pressure reaches a maximum, dust particles drift outwards, possibly overcoming their coupling to the inward accreting gas. Dust particles will then remain at the gap's outer edge while the gas flows through the gap. This process is called "dust filtration" (*Rice et al.* 2006), and it depletes dust interior to the semi-major axis of the planet-induced gap, forming a dust-depleted inner disk.

Dust trapping at the gap edge was first simulated by *Paardekooper and Mellema* (2006); *Fouchet et al.* (2007). However, without considering particle diffusion due to disk turbulence, mm and cm sized particles will drift from tens of AU into the star within 200 orbits. *Zhu et al.* (2012) included particle diffusion due to disk turbulence in 2-D simulations evolving over viscous timescales, where a quasi-steady state for both gas and dust has been achieved, and found that micron sized particles are difficult to filter by a Jupiter mass planet in a $\dot{M} = 10^{-8} M_\odot\, yr^{-1}$ disk. *Pinilla et al.* (2012) has done 1-D calculations considering dust growth and dust fragmentation at the gap edge and suggested that micron-sized particles may also be filtered. Considering the flow pattern is highly asymmetric within the gap, 2-D simulations including both dust growth and dust fragmentation may be needed to better understand the dust filtration process.

Dust filtration suggests that a deeper gap opened by a more massive planet can lead to the depletion of smaller dust particles. Thus transitional disks may have a higher mass planet(s) than pre-transitional disks. Since a higher mass planet exerts a stronger torque on the outer disk, it may slow down the accretion flow passing the planet and lead to a lower disk accretion rate onto the star. This is consistent with observations that transitional disks have lower accretion rates than pre-transitional disks (*Espaillat et al.* 2012; *Kim et al.* 2013). Furthermore, dust filtration can explain the observed differences in the relative distributions of micron sized dust grains and mm sized dust grains. Disks where the small dust grains appear to closely trace the large dust distribution (i.e., category C disks from §2.3) could be in an advanced stage of dust filtration, after the dust grains in the inner disk have grown to larger sizes and can no longer be detected in NIR scattered light. Disks with NIR scattered light imaging evidence for a significant amount of small, submicron sized dust grains within the cavities in the large, mm-sized dust grains seen in the submm (i.e., the category A and C disks from §2.3), could be in an earlier stage of disk clearing via dust filtration.

Future observations will further our understanding of the many physical processes which can occur when a giant planet is in a disk, such as dust growth in the inner disk, dust growth at the gap edge (*Pinilla et al.* 2012), tidal stripping

of the planets (*Nayakshin* 2013), and planets in the dead zone (*Morishima* 2012; *Bae et al.* 2013b). In addition, here we have explored how to explain large holes and gaps in disks, yet there may be smaller gaps present in disks (§ 2.1) that may not be observable with current techniques. The gap opening process is tied to the viscosity parameter assumed. If the disk is inviscid, a very low mass perturber can also open a small gap (e.g., 10 $M_{\oplus}$; *Li et al.* 2009; *Muto et al.* 2010; *Duffell and MacFadyen* 2012; *Zhu et al.* 2013; *Fung et al.* 2014). Disk ionization structure calculations have indeed suggested the existence of such low turbulence regions in protoplanetary disks (i.e., the dead zone, see chapter by *Turner et al.* in this volume), which may indicate that gaps in disks are common. Interestingly, in a low viscosity disk, vortices can also be produced at the gap edge (*Li et al.* 2005), which can efficiently trap dust particles (Fig. 10; *Lyra et al.* 2009; *Ataiee et al.* 2013; *Lyra and Lin* 2013, *Zhu et al.*, in press) and is observable with ALMA (*van der Marel et al.* 2013). We note that other physical processes can also induce vortices (see chapter by *Turner et al.* in this volume; *Klahr and Henning* 1997; *Wolf and Klahr* 2002), thus the presence of vortices cannot be viewed as certain evidence for the presence of a planet within a disk gap. In the near future, new observations with ALMA will provide further constraints on the distributions of dust and gas in the disk, which will help illuminate our understanding of the above points.

4. DEMOGRAPHICS

Basic unresolved questions underlie and motivate the study of disk demographics around TTS. Do all disks go through a (pre-)transitional disk phase as stars evolve from disk-bearing stars to diskless stars? Assuming an affirmative answer, we can measure a *transition timescale* by multiplying the fraction of disk sources with (pre-)transitional disk SEDs with the TTS disk lifetime (*Skrutskie et al.* 1990). Are (pre-)transitional disks created by a single process or multiple processes? Theory predicts that several mechanisms can generate (pre-)transitional disk SEDs, all of which are important for disk evolution. Table 2 summarizes the generic properties expected for (pre-)transitional disks produced by different mechanisms, as previously described in § 3 and the literature (e.g., *Najita et al.* 2007a; *Alexander and Armitage* 2007). Which of these occur commonly (or efficiently) and on what timescale(s)? These questions can, in principle, be addressed demographically because different mechanisms are predicted to occur more readily in different kinds of systems (e.g., those of different disk masses and ages) and are expected to impact system parameters beyond the SED (e.g., the stellar accretion rate). We highlight developments along these lines below, taking into account points raised in §2 and 3.

4.1 Frequency and the Transition Timescale

Because different clearing mechanisms likely operate on different timescales, demographic studies aim to identify the processes that produce (pre-)transitional disks in populations of different ages. One area that has been investigated thoroughly is the overall frequency of transitional disks. *Spitzer* surveys have had tremendous success in cataloging young stellar object (YSO) populations, identifying dust emission from disks around stars within 500 pc across the full stellar mass range and into the brown dwarf regime at 3.6 to 8 μm, and for most of the stellar mass range at 24 μm. Based on the photometric SEDs, a number of studies have identified transitional disk candidates, allowing demographic comparisons with stellar and disk properties. We note that reported transitional disk frequencies to date should be taken as a lower limit on the frequency of holes and gaps in disks given that, as noted in § 2.1, it is harder to identify pre-transitional disks based on photometry alone as well as smaller gaps in disks with current data.

There has been some controversy regarding the transition timescale, which as noted above can be estimated from the frequency of transitional disks relative to the typical disk lifetime. Early pre-*Spitzer* studies (e.g., *Skrutskie et al.* 1990; *Wolk and Walter* 1996) suggested that the transition timescale was short, of order 10% of the total disk lifetime, a few 10^5 years. The values estimated from *Spitzer* surveys of individual clusters/star forming regions have a wider range, from as small as these initial estimates (*Cieza et al.* 2007; *Hernández et al.* 2007b; *Luhman et al.* 2010; *Koepferl et al.* 2013) to as long as a time comparable to the disk lifetime itself (*Currie et al.* 2009; *Sicilia-Aguilar et al.* 2009; *Currie and Sicilia-Aguilar* 2011). Combining data from multiple regions, *Muzerolle et al.* (2010) found evidence for an increase in the transitional disk frequency as a function of mean cluster age.

The discrepancies among these studies are largely the result of differing definitions of what constitutes a disk in transition, as well as how to estimate the total disk lifetime. The shorter timescales are typically derived using more restrictive selection criteria. In particular, the evolved disks, in which the IR excess is small at all observed wavelengths, tend to be more common around older stars ($\gtrsim$ 3 Myr) and low-mass stars and brown dwarfs; the inclusion of this SED type will lead to a larger transitional disk frequency and hence timescale for samples that are heavily weighted to these stellar types. Moreover, the status of the evolved disks as *bona fide* (pre-)transitional disks (i.e., a disk with inner clearing) is somewhat in dispute (see § 2.1). As pointed out by *Najita et al.* (2007a), the different SED types may indicate multiple evolutionary mechanisms for disks. More complete measurements of disk masses, accretion rates, and resolved observations of these objects are needed to better define their properties and determine their evolutionary status.

Combining data from multiple regions and restricting the selection to transitional disk SEDs showing evidence for inner holes, *Muzerolle et al.* (2010) found evidence for an increase in the transition frequency as a function of mean

TABLE 2
OBSERVABLE CHARACTERISTICS OF PROPOSED DISK CLEARING MECHANISMS

Mechanism	Dust Distribution	Gas Distribution	Accretion Rate	Disk Mass	L_X
Viscous evolution	No hole/gap	No hole/gap	Low accretion	Low mass	No dependence
Grain growth	No hole/gap	No hole/gap	Unchanged	All masses	No dependence
Photoevaporation	R_h-radius hole	No/little gas within R_h	No/low accretion	Low mass	Correlated
$\sim$0.1 M_J planet	Gap	No hole/gap	Unchanged	All masses	No dependence
$\sim$1 M_J planet	Gap	Gap	$\sim 0.1 - 0.9$ CTTS	Higher masses[a]	No dependence
Multiple giant planets	Gap/R_h-radius hole	No/little gas within R_h	No/low accretion	Higher masses[a]	No dependence

NOTE.—Here we refer to the dust and gas distribution of the inner disk. Relative terms are in comparison to the properties of otherwise comparable disks around CTTS (e.g., objects of similar age, mass). [a]Higher mass disks may form planets easier according to core accretion theory (see chapter in this volume by *Helled et al.*). Observations are needed to test this.

cluster age. However, there was considerable uncertainty because of the small number statistics involved, especially at older ages where the total disk frequency is typically 10% or less. Fig. 11 shows the fraction of transitional disks relative to the total disk population in a given region as a function of the mean age of each region. Here we supplement the statistics from the IRAC/MIPS flux-limited photometric surveys listed in *Muzerolle et al.* (2010) with new results from IRS studies of several star forming regions (*McClure et al.* 2010; *Oliveira et al.* 2010; *Furlan et al.* 2011; *Manoj et al.* 2011; *Arnold et al.* 2012a), and a photometric survey of the 11 Myr-old Upper Scorpius association (*Luhman and Mamajek* 2012). A weak age dependence remains, with frequencies of a few percent at t $\lesssim$ 2 Myr and $\sim$10 percent at older ages. Some of this correlation can be explained as a consequence of the cessation of star formation in most regions after $\sim$ 3 Myr; as *Luhman et al.* (2010) noted, the frequency of transitional disks relative to full disks in a region no longer producing new disks should increase as the number of full disks decreases with time. Note that the sample selection does not include pre-transitional disks, which cannot be reliably identified without MIR spectroscopy. Interestingly, for the regions with reasonably complete IRS observations (the four youngest regions in Fig. 11), the transition fraction would increase to $\sim 10 - 15$% if the pre-transitional disks were included. Note also that the IRS surveys represent the known membership of each region, and are reasonably complete down to spectral types of about M5. We refer the reader to the cited articles for a full assessment of sample completeness. All transitional disks in this combined sample are spectroscopically confirmed PMS stars.

An important caveat to the above statistics is that SED morphology is an imperfect tracer of disk structure and is most sensitive to large structures that span many AU (see § 2.1). Smaller gaps can be masked by emission from even tiny amounts of dust. As mentioned in § 2.2, resolved submillimeter imaging has found a greater frequency of disks with inner dust cavities among the 1-2 Myr-old stars in Taurus and Ophiuchus ($\sim$30%; *Andrews et al.* 2011b) than has been estimated from NIR flux deficits alone. The statistics for older regions are incomplete, limited by weaker (sub)millimeter emission that may be a result of significant grain growth compared to younger disks (*Lee et al.* 2011; *Mathews et al.* 2012). Improved statistics await more sensitive observations such as with ALMA.

4.2 Disk Masses and Accretion Rates

Another powerful tool has been to compare stellar accretion rates and total disk mass. Looking at full disks around CTTS and (pre-)transitional disks in Taurus, *Najita et al.* (2007a) found that compared to single CTTS, (pre-)transitional disks have stellar accretion rates $\sim$ 10 times lower at the same disk mass and median disk masses $\sim$ 4 times larger. These properties are roughly consistent with the expectations for Jupiter mass giant planet formation. Some of the low accretion rate, low disk mass sources could plausibly be produced by UV photoevaporation, although none of the (pre-)transitional disks (GM Aur, DM Tau, LkCa 15, UX Tau A) are in this group. Notably, none of these disks were found to overlap the region of the $\dot{M}_*$–M_d plane occupied by most disks around CTTS.

With the benefit of work in the literature, a preliminary $\dot{M}_*$–M_d plot can also be made for disks around CTTS and (pre-)transitional disks in Ophiuchus (Fig. 12). Most of the Oph sources are co-located with the Taurus CTTS, while several fall below this group. The latter includes DoAr 25 and the transitional disk SR 21 . The other two sources have high extinction. Such sources ($A_v > 14$; Fig. 12, blue squares) are found to have lower $\dot{M}_*$, on average, for their disk masses. This is as might be expected, if scattered light leads to an underestimate of A_v, and therefore the line luminosity from which $\dot{M}_*$ is derived. A source like DoAr 25, which has a very low accretion rate for its disk mass and also lacks an obvious hole based on the SED or submillimeter continuum imaging (*Andrews and Williams* 2008; *Andrews et al.* 2009, 2010), is interesting. Does it have a smaller gap than can be measured with current techniques? Higher angular resolution observations of such sources could explore this possibility.

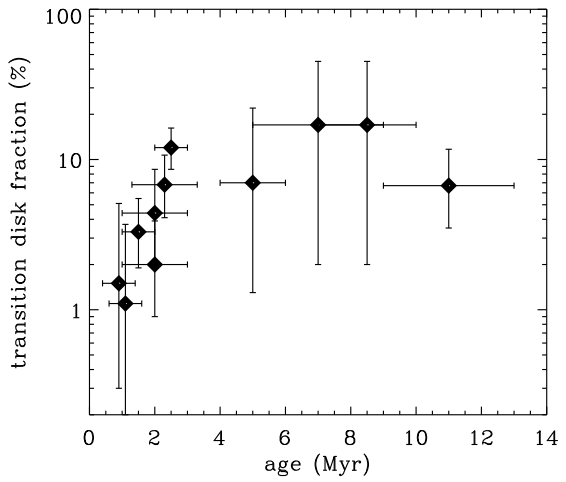

Fig. 11.— The transitional disk fraction for ten star-forming regions and young clusters as a function of mean stellar age. Fractions were estimated by taking the ratio of the number of objects that exhibit a transitional disk SED with the total number of disks in each region. Evolved disks and pre-transitional disks are not included here. The data are taken from (in order of mean age): *Arnold et al.* (2012a), NGC 1333; *McClure et al.* (2010), Ophiuchus; *Furlan et al.* (2011), Taurus; *Manoj et al.* (2011), Chamaeleon I; *Flaherty and Muzerolle* (2008), NGC 2068/2071; *Oliveira et al.* (2010), Serpens; *Muench et al.* (2007), IC 348; *Hernández et al.* (2007a), Orion OB1a/b; *Megeath et al.* (2005), η Chamaeleontis association; *Luhman and Mamajek* (2012), Upper Scorpius association.

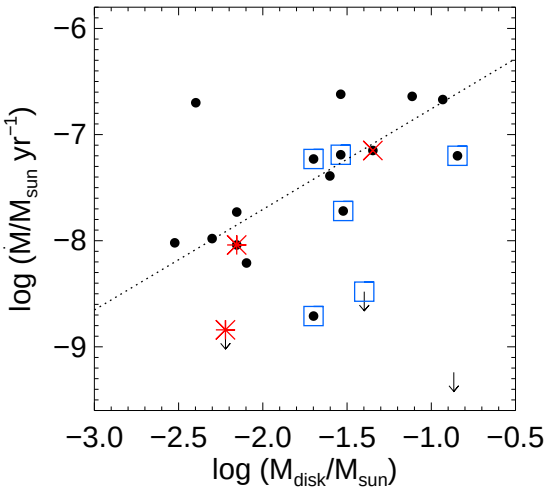

Fig. 12.— Preliminary $\dot{M}_*$–M_d for disks in Ophiuchus. The dotted line indicates the locus occupied by CTTS in Taurus (*Najita et al.* 2007a). Disks with submm cavities and (pre-)transitional disk SEDs are overlaid with a star (SR 21, bottom left; DoAr 44, middle); the disk with a submm cavity but no obvious SED MIR deficit (SR 24S) is overlaid with an "X" . Sources with A_V>14 (*McClure et al.* 2010) are indicated with a blue box. Objects where only upper limits were available for the accretion rates are indicated with an arrow (including SR 21, GSS 26, DoAr 25). Accretion rates are from *Natta et al.* (2006) if available, otherwise from *Eisner et al.* (2005), and *Valenti et al.* (1993) (scaled). Disk masses are from *Andrews and Williams* (2007); *Andrews et al.* (2010).

Like SR 21, both SR 24S and DoAr 44 have also been identified as having cavities in their submillimeter continuum (*Andrews et al.* 2011b), although their accretion rates place them in the CTTS region of the plot. DoAr 44 has been previously identified as a pre-transitional disk based on its SED (*Espaillat et al.* 2010). Whether SR 24S has a strong MIR deficit in its SED is unknown, as its SED has not been studied in as much detail.

What accounts for the CTTS-like accretion rates of these systems? One possibility is that these systems may be undergoing low mass planet formation. Several studies have described how low mass planets can potentially clear gaps in the dust disk while having little impact on the gas, with the effect more pronounced for the larger grains probed in the submillimeter (see § 3.2, also *Paardekooper and Mellema* 2006; *Fouchet et al.* 2007).

In related work, recent studies find that (pre-)transitional disks have lower stellar accretion rates on average than other disks in the same star forming region and that the accretion rates of pre-transitional disks are closer to that of CTTS than the transitional disks (*Espaillat et al.* 2012; *Kim et al.* 2013). However, other studies find little difference between the accretion rates of (pre-)transitional and other disks (*Keane et al.*, submitted; *Fang et al.* 2013). This could be due to different sample selection (i.e., colors vs. IRS spectra) and/or different methods for calculating accretion rates (i.e., H_α vs. NIR emission lines). More work has to be done to better understand disk accretion rates, ideally with a large IR and submm selected sample and consistent accretion rate measurement methods.

4.3 Stellar Host Properties

One would naively expect an age progression from full disks to (pre-)transitional disks to diskless stars in a given region if these classes represent an evolutionary sequence. Observational evidence for age differences, however, is decidedly mixed. From improved parallax measurements in Taurus, *Bertout et al.* (2007) found that the four stars surrounded by (pre-)transitional disks with age measurements (DM Tau, GM Aur, LkCa 15, UX Tau A) were intermediate between the mean CTTS and weak TTS (i.e., stars that are not accreting) ages. However, the quoted age uncertainties are roughly equal to the ages of individual objects, and the small sample is not statistically robust. Moreover, studies of other regions have found no statistical difference in ages between stars with and without disks (NGC 2264, Orion; *Dahm and Simon* 2005; *Jeffries et al.* 2011). In general, the uncertainties associated with determining stellar ages remain too large, and the samples of (pre-)transitional disks too small, to allow any definitive conclusion of systematic

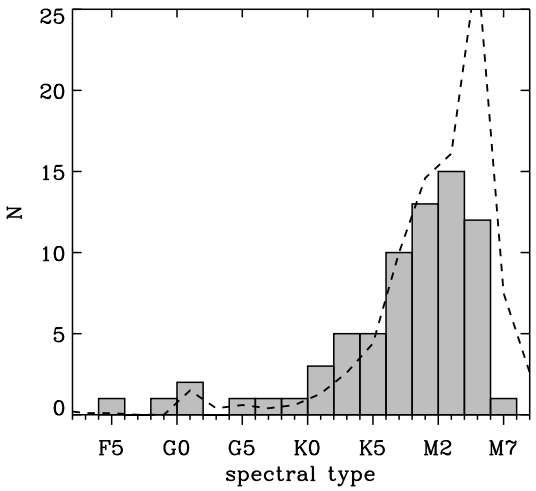

Fig. 13.— The distribution of spectral types for the known transitional disks with spectral type F5 or later. The dashed line indicates the combined parent sample of all disks in the 1–3 Myr old regions, scaled down by a factor of 10, highlighting the apparent deficit of transitional disks around stars later than ∼M4.

age differences for (pre-)transitional disks.

The frequency of transitional disks as a function of stellar mass also provides some clues to their origins. *Muzerolle et al.* (2010) showed that transitional disks appeared to be underrepresented among mid- to late-M stars compared with the typical initial mass function of young stellar clusters. Using the expanded sample adopted for Fig. 11, this initial finding appears to be robust (Fig. 13). The deficit remains even after adding the known pre-transitional disks. However, the evolved disks (as opposed to the *transitional* disks) do appear to be much more common around lower-mass stars (e.g., *Sicilia-Aguilar et al.* 2008). As *Ercolano et al.* (2009) pointed out, there may be a strong bias here as optically thick inner disks around mid- to late-M stars produce less short-wavelength excess and can be confused with true inner disk clearing. Nevertheless, this discrepancy may provide another indication of different clearing mechanisms operating in different transitional disks. For example, the relative dearth of (pre-)transitional disks around lower mass stars may reflect a decreased rate of giant planet formation, as would be expected given their typically smaller initial disk masses.

Among other stellar properties, the X-ray luminosity can provide further useful constraints. L_X has been invoked as a major contributor to theoretical photoevaporation rates (e.g., *Gorti and Hollenbach* 2009; *Owen et al.* 2012), as well as accretion rates related to MRI at the inner disk edge (*Chiang and Murray-Clay* 2007). Examining the (pre-)transitional disks in Taurus and Chamaleon I, *Kim et al.* (2009) found correlations between the size of the inner cleared regions and several stellar/disk properties including stellar mass, X-ray luminosity, and mass accretion rate. These possibly point to the MRI or photoevaporation mechanisms. However, known independent correlations between stellar mass, L_X, and mass accretion rate may also be responsible. In a follow-up study with a large sample of 62 (pre-)transitional disks in Orion, *Kim et al.* (2013) attempted to correct for the stellar mass dependences and found no residual correlation between accretion rate or L_X and the size of the inner hole. The measured properties of most (pre-)transitional disks do not overlap with the ranges of parameter space predicted by these models. *Kim et al.* (2013) concluded that the demographics of their sample are most consistent with giant planet formation being the dominant process responsible for creating (pre-)transitional disk SEDs.

To better understand the connection between underlying physical mechanisms and observed disk demographics, more theoretical and observational work needs to be done. Improved theoretical estimates on stellar ages, accretion efficiencies, and disk masses for different clearing mechanisms will aid in interpretation of the observations. At the same time, larger ground-based surveys are essential to confidently constrain basic properties such as stellar accretion rates, ages, and disk masses. In the near future, the higher resolution of ALMA will reveal the extent of gaps in disks, leading to better statistics to measure the (pre-)transitional disk frequency and the transition timescale. *JWST* will be key in addressing how the (pre-)transitional frequency depends on age. The best constraints on disk demographics clearly require a multi-wavelength approach.

5. CONCLUDING REMARKS AND FUTURE PROSPECTS

It is thought that practically all stars have planets (see chapter in this volume by *Fischer et al.*). If we start with the reasonable assumption that these planets formed out of disks, then the question is not if there are planets in disks around young stars, but what are their observable signatures. To date we have detected large, optically thin holes and gaps in the dust distribution of disks and theoretical planet clearing mechanisms can account for some of their observed properties. These (pre-)transitional disks have captured the interest of many scientists since they may be a key piece of evidence in answering one of the fundamental questions in astronomy: how do planets form?

While other disk clearing mechanisms (e.g, grain growth, photoevaporation; § 3.1) should certainly be at play in most, if not all, disks (and may even work more effectively in concert with planets; *Rosotti et al.* 2013), here we speculate what kinds of planets could be clearing (pre-)transitional disks, beginning with massive giant planets. If a massive giant planet (or multiple planets) is forming in a disk, it will cause a large cavity in the inner disk since it will be very efficient at cutting off the inner disk from the outer disk. This will lead to significant depletion of small and large dust grains in the inner disk and lower accretion onto the central

star (§ 3.2). This is consistent with (pre-)transitional disks which have submm and NIR scattered light cavities and MIR deficits in the SED (e.g., LkCa 15, GM Aur, Sz 91, RX J1604-2130; § 2.1–2.3). This is also consistent with the lower accretion rates measured for these objects (§ 4.2). One caveat is that massive planets would be the easiest to detect, yet there has not been a robust detection of a protoplanet in a (pre-)transitional disk yet.

A less massive planet (or fewer planets) would still lead to substantial clearing of the inner disk, but be less efficient at cutting off the inward flow of material from the outer disk (§ 3.2). This is consistent with those (pre-)transitional disks that have a submm cavity but no MIR deficit in the SED, such as WSB 60, indicating that small dust still makes it through into the inner disk (§ 2.1–2.3). Interestingly, WSB 60 is in Oph and overall (pre-)transitional disks SEDs are rare in this region. Given that Oph is quite young (age ~ 1 Myr), this may be indicative of the effects of dust evolution and/or planet growth. Disks in Oph could be in the initial stages of gap opening by planets whereas in older systems, the dust grains in the inner disk have grown to larger sizes and/or the planets have grown large enough to more efficiently disrupt the flow of material into the inner disk. The above suggests that most disks with planets go through a pre-transitional disk phase and that there are many disks with small gaps that have escaped detection with currently available techniques. More theoretical work is needed to explore if all pre-transitional disks eventually enter a transitional disk phase as planets grow more massive and the inner disk is accreted onto the star. Note also that there are some disks which have submm cavities and MIR SED deficits, but no evidence of clearing in NIR scattered light (e.g., SR 21, DoAr 44, RX J1615−3255). Apparently, there is some important disk physics regarding accretion efficiencies that we are missing. It is necessary to study disks in other star forming regions with ALMA, both to probe a range of ages and to increase the statistical sample size, in order to address questions of this kind. Detections of protoplanets would be ideal to test the link between planet mass and disk structure.

While much progress has been made understanding the nature of the disks described above, future work may focus more closely on disks with smaller optically thin gaps that could plausibly be created by low-mass planets. The presence of low mass orbiting companions ($\sim 0.1 M_J$; *Paardekooper and Mellema* 2006) is expected to alter the dust disk significantly with little impact on the gas disk, whereas high mass companions ($\gtrsim 1 M_J$) can create gaps or holes in the gas disk and possibly alter its dynamics. *Kepler* finds that super-earth mass objects are very common in mature planetary systems (see chapter in this volume by *Fischer et al.*), so it may be that smaller mass objects form fairly commonly in disks and open holes and gaps that are not cleared of dust. These systems are more difficult to identify with SED studies and current interferometers, so potentially there are many more disks with gaps than currently known. High spatial resolution images from ALMA will be able to detect these small gaps, in some cases even those with sizes down to about 3 AU (*Wolf and D'Angelo* 2005; *Gonzalez et al.* 2012).

There are many remaining avenues that researchers can take to fully characterize clearing in disks around TTS. Theoretically, we can simulate the influence of various mass planets on different sized dust particles, which can be compared with observations at various wavelengths to constrain a potential planet's mass. We can use ALMA, VLTI, and JWST to test the full extent of disk holes and gaps as well as their frequency with respect to age. We can also make substantial progress studying the gas distributions in disks in the near future with ALMA, particularly to determine if the structure inferred for the disk from studies of the dust is the same as that in the gas. Gas tracers may also reveal the presence of an orbiting planet via emission from a circumplanetary disk. Lastly, and perhaps most importantly, we need robust detections of protoplanets in disks around young stars. These future advances will help us understand how gas/ice giant planets and terrestrial planets form out of disks and hopefully antiquate this review by the time of PPVII.

Acknowledgments. The authors thank the anonymous referee, C. Dullemond, L. Hartmann, and L. Ingleby for insightful comments which helped improve this review. Work by C.E. was performed in part under contract with Caltech funded by NASA through the Sagan Fellowship Program executed by the NASA Exoplanet Science Institute. Z.Z. acknowledges support by NASA through Hubble Fellowship grant HST-HF-51333.01-A awarded by the Space Telescope Science Institute, which is operated by the Association of Universities for Research in Astronomy, Inc., for NASA, under contract NAS 5-26555.

Finally, a special recognition of the contribution of Paola D'Alessio, who passed away in November of 2013. She is greatly missed as a scientist, colleague, and friend.

Among Paola's most important papers are those which addressed the issue of dust growth and mixing in T Tauri disks. In *D'Alessio et al.* (1999), she showed that disk models with well-mixed dust with properties like that of the diffuse interstellar medium produced disks that were too vertically thick and produced too much infrared excess, while lacking sufficient mm-wave fluxes. In the second paper of the series (*D'Alessio et al.* 2001) Paola and collaborators showed that models with power-law size distributions of dust with maximum sizes around 1 mm produced much better agreement with the mm and infrared emission of most T Tauri disks, but failed to exhibit the 10 μm silicate emission feature usually seen, leading to the conclusion that the large grains must have settled closer to the midplane while leaving a population of small dust suspended in the upper disk atmosphere. This paper provided the first clear empirical evidence for the expected evolution of dust as a step in growing larger bodies in protoplanetary disks. Another important result was the demonstration that once grain growth

proceeds past sizes comparable to the wavelengths of observation, the spectral index of the disk emission is determined only by the size distribution of the dust, not its maximum. Along with quantitative calculations of dust properties, the results imply that the typical opacities used to estimate dust masses will generally lead to underestimates of the total solid mass present, a point that is frequently forgotten or ignored.

In the third paper of this series (*D'Alessio et al.* 2006), Paola and her collaborators developed models which incorporated a thin central layer of large dust along with depleted upper disk layers containing small dust. The code which developed these models has been used in over 30 papers to compare with observations, especially those from the Infrared Spectrograph (IRS) (*Furlan et al.* 2005; *McClure et al.* 2010) as well as the IRAC camera (*Allen et al.* 2004) on board the Spitzer Space Telescope, and more recently from PACS on board the Herschel Space Telescope (*McClure et al.* 2012), and from the SMA (*Qi et al.* 2011).

Paola's models also played a crucial role in the recognition of transitional and pre-transitional T Tauri disks (*Calvet et al.* 2002; *D'Alessio et al.* 2005; *Espaillat et al.* 2007, 2010). In many cases, particularly those of the pre-transitional disks, finding evidence for an inner hole or gap from the spectral energy distribution depends upon careful and detailed modeling. The inference of gaps and holes from the SEDs is now being increasingly confirmed directly by mm- and sub-mm imaging (*Hughes et al.* 2009), showing reasonable agreement in most cases with the hole sizes predicted by the models. Combining imaging with SED modeling in the future will place additional constraints on the properties of dust in protoplanetary disks.

Paola's influence in the community extended well beyond her direct contributions to the literature in over 100 refereed papers. She provided disk models for many other researchers as well as detailed dust opacities. The insight provided by her calculations informed many other investigations, as studies of X-ray heating of protoplanetary disk atmospheres (*Glassgold et al.* 2004, 2007, 2009), of the chemical structure of protoplanetary disks and propagation of high energy radiation (*Fogel et al.* 2011; *Bethell and Bergin* 2011) and on the photoevaporation of protoplanetary disks (*Ercolano et al.* 2008).

Paola's passing is a great loss to the star formation community and we remain grateful for her contributions to our field.

REFERENCES

Acke B. and van den Ancker M. E. (2006) *Astron. Astrophys.*, *449*, 267.

Aguilar L. A. et al. (2008) in: *Revista Mexicana de Astronomia y Astrofisica Conference Series*, vol. 34 of *Revista Mexicana de Astronomia y Astrofisica Conference Series*, pp. 91–97.

Akeson R. L. et al. (2011) *Astrophys. J.*, *728*, 96.

Alcalá J. M. et al. (2014) *Astron. Astrophys.*, *561*, A2.

Alexander R. D. and Armitage P. J. (2007) *Mon. Not. R. Astron. Soc.*, *375*, 500.

Alexander R. D. and Armitage P. J. (2009) *Astrophys. J.*, *704*, 989.

Alexander R. D. et al. (2006) *Mon. Not. R. Astron. Soc.*, *369*, 229.

Allen L. E. et al. (2004) *Astrophys. J. Suppl.*, *154*, 363.

Andrews S. M. and Williams J. P. (2007) *Astrophys. J.*, *659*, 705.

Andrews S. M. and Williams J. P. (2008) *Astrophys. Space Sci.*, *313*, 119.

Andrews S. M. et al. (2009) *Astrophys. J.*, *700*, 1502.

Andrews S. M. et al. (2010) *Astrophys. J.*, *723*, 1241.

Andrews S. M. et al. (2011a) *Astrophys. J. Lett.*, *742*, L5.

Andrews S. M. et al. (2011b) *Astrophys. J.*, *732*, 42.

Arnold L. A. et al. (2012a) *Astrophys. J. Suppl.*, *201*, 12.

Arnold T. J. et al. (2012b) *Astrophys. J.*, *750*, 119.

Artymowicz P. and Lubow S. H. (1994) *Astrophys. J.*, *421*, 651.

Ataiee S. et al. (2013) *Astron. Astrophys.*, *553*, L3.

Avenhaus H. et al. (2014) *Astrophys. J.*, *781*, 87.

Bae J. et al. (2013a) *Astrophys. J.*, *774*, 57.

Bae J. et al. (2013b) *Astrophys. J.*, *764*, 141.

Beckwith S. V. W. et al. (1990) *Astron. J.*, *99*, 924.

Benisty M. et al. (2010) *Astron. Astrophys.*, *511*, A75.

Bertout C. et al. (2007) *Astron. Astrophys.*, *473*, L21.

Bethell T. J. and Bergin E. A. (2011) *Astrophys. J.*, *740*, 7.

Biller B. et al. (2012) *Astrophys. J. Lett.*, *753*, L38.

Birnstiel T. et al. (2012) *Astron. Astrophys.*, *544*, A79.

Birnstiel T. et al. (2013) *Astron. Astrophys.*, *550*, L8.

Bouwman J. et al. (2003) *Astron. Astrophys.*, *401*, 577.

Brauer F. et al. (2008) *Astron. Astrophys.*, *480*, 859.

Brittain S. D. et al. (2007) *Astrophys. J.*, *659*, 685.

Brittain S. D. et al. (2009) *Astrophys. J.*, *702*, 85.

Brittain S. D. et al. (2013) *Astrophys. J.*, *767*, 159.

Brown J. M. et al. (2007) *Astrophys. J. Lett.*, *664*, L107.

Brown J. M. et al. (2008) *Astrophys. J. Lett.*, *675*, L109.

Brown J. M. et al. (2009) *Astrophys. J.*, *704*, 496.

Brown J. M. et al. (2012) *Astrophys. J. Lett.*, *758*, L30.

Bruderer S. et al. (2014) *Astron. Astrophys.*, *562*, A26.

Calvet N. et al. (2000) *Protostars and Planets IV*, p. 377.

Calvet N. et al. (2002) *Astrophys. J.*, *568*, 1008.

Calvet N. et al. (2004) *Astron. J.*, *128*, 1294.

Calvet N. et al. (2005) *Astrophys. J. Lett.*, *630*, L185.

Carpenter J. M. et al. (2001) *Astron. J.*, *121*, 3160.

Casassus S. et al. (2012) *Astrophys. J. Lett.*, *754*, L31.

Casassus S. et al. (2013) *Nature*, *493*, 191.

Chiang E. and Murray-Clay R. (2007) *Nature Physics*, *3*, 604.

Cieza L. et al. (2007) *Astrophys. J.*, *667*, 308.

Cieza L. A. et al. (2010) *Astrophys. J.*, *712*, 925.

Cieza L. A. et al. (2012) *Astrophys. J.*, *752*, 75.

Cieza L. A. et al. (2013) *Astrophys. J. Lett.*, *762*, L12.

Clarke C. J. et al. (2001) *Mon. Not. R. Astron. Soc.*, *328*, 485.

Close L. M. et al. (2014) *Astrophys. J. Lett.*, *781*, L30.

Cohen M. and Kuhi L. V. (1979) *Astrophys. J. Suppl.*, *41*, 743.

Crida A. et al. (2006) *Icarus*, *181*, 587.

Currie T. and Sicilia-Aguilar A. (2011) *Astrophys. J.*, *732*, 24.

Currie T. et al. (2009) *Astrophys. J.*, *698*, 1.

Dahm S. E. and Simon T. (2005) *Astron. J.*, *129*, 829.

D'Alessio P. et al. (1999) *Astrophys. J.*, *527*, 893.

D'Alessio P. et al. (2001) *Astrophys. J.*, *553*, 321.

D'Alessio P. et al. (2005) *Astrophys. J.*, *621*, 461.

D'Alessio P. et al. (2006) *Astrophys. J.*, *638*, 314.

de Juan Ovelar M. et al. (2013) *Astron. Astrophys.*, *560*, A111.

Debes J. H. et al. (2013) *Astrophys. J.*, *771*, 45.

Dodson-Robinson S. E. and Salyk C. (2011) *Astrophys. J.*, *738*, 131.

Donati J.-F. et al. (2011) *Mon. Not. R. Astron. Soc.*, *417*, 1747.

Dong R. et al. (2012) *Astrophys. J.*, *760*, 111.
Draine B. T. (2006) *Astrophys. J.*, *636*, 1114.
Duffell P. C. and MacFadyen A. I. (2012) *Astrophys. J.*, *755*, 7.
Dullemond C. P. and Dominik C. (2005) *Astron. Astrophys.*, *434*, 971.
Durisen R. H. et al. (2007) in: *Protostars and Planets V*, (edited by B. Reipurth, D. Jewitt, and K. Keil), pp. 607–622.
Dutrey A. et al. (2008) *Astron. Astrophys.*, *490*, L15.
Eisner J. A. et al. (2005) *Astrophys. J.*, *623*, 952.
Eisner J. A. et al. (2006) *Astrophys. J. Lett.*, *637*, L133.
Ercolano B. et al. (2008) *Astrophys. J.*, *688*, 398.
Ercolano B. et al. (2009) *Astrophys. J.*, *699*, 1639.
Espaillat C. et al. (2007) *Astrophys. J. Lett.*, *670*, L135.
Espaillat C. et al. (2008a) *Astrophys. J. Lett.*, *689*, L145.
Espaillat C. et al. (2008b) *Astrophys. J. Lett.*, *682*, L125.
Espaillat C. et al. (2010) *Astrophys. J.*, *717*, 441.
Espaillat C. et al. (2011) *Astrophys. J.*, *728*, 49.
Espaillat C. et al. (2012) *Astrophys. J.*, *747*, 103.
Evans T. M. et al. (2012) *Astrophys. J.*, *744*, 120.
Fang M. et al. (2013) *Astrophys. J. Suppl.*, *207*, 5.
Feigelson E. et al. (2007) in: *Protostars and Planets V*, (edited by B. Reipurth, D. Jewitt, and K. Keil), pp. 313–328.
Flaherty K. M. and Muzerolle J. (2008) *Astron. J.*, *135*, 966.
Flaherty K. M. et al. (2011) *Astrophys. J.*, *732*, 83.
Flaherty K. M. et al. (2012) *Astrophys. J.*, *748*, 71.
Fogel J. K. J. et al. (2011) *Astrophys. J.*, *726*, 29.
Follette K. B. et al. (2013) *Astrophys. J.*, *767*, 10.
Fouchet L. et al. (2007) *Astron. Astrophys.*, *474*, 1037.
France K. et al. (2012) *Astrophys. J.*, *756*, 171.
Fung J. et al. (2014) *Astrophys. J.*, *782*, 88.
Furlan E. et al. (2005) *Astrophys. J. Lett.*, *628*, L65.
Furlan E. et al. (2011) *Astrophys. J. Suppl.*, *195*, 3.
Geers V. C. et al. (2007) *Astron. Astrophys.*, *469*, L35.
Glassgold A. E. et al. (2004) *Astrophys. J.*, *615*, 972.
Glassgold A. E. et al. (2007) *Astrophys. J.*, *656*, 515.
Glassgold A. E. et al. (2009) *Astrophys. J.*, *701*, 142.
Gonzalez J.-F. et al. (2012) *Astron. Astrophys.*, *547*, A58.
Goodson A. P. and Winglee R. M. (1999) *Astrophys. J.*, *524*, 159.
Gorti U. and Hollenbach D. (2009) *Astrophys. J.*, *690*, 1539.
Gorti U. et al. (2009) *Astrophys. J.*, *705*, 1237.
Goto M. et al. (2006) *Astrophys. J.*, *652*, 758.
Grady C. A. et al. (2001) *Astron. J.*, *122*, 3396.
Grady C. A. et al. (2013) *Astrophys. J.*, *762*, 48.
Guilloteau S. and Dutrey A. (1994) *Astron. Astrophys.*, *291*, L23.
Guilloteau S. et al. (2011) *Astron. Astrophys.*, *529*, A105.
Habart E. et al. (2006) *Astron. Astrophys.*, *449*, 1067.
Hartmann L. et al. (1998) *Astrophys. J.*, *495*, 385.
Hartmann L. et al. (2006) *Astrophys. J.*, *648*, 484.
Hashimoto J. et al. (2011) *Astrophys. J. Lett.*, *729*, L17.
Hashimoto J. et al. (2012) *Astrophys. J. Lett.*, *758*, L19.
Hernández J. et al. (2007a) *Astrophys. J.*, *662*, 1067.
Hernández J. et al. (2007b) *Astrophys. J.*, *671*, 1784.
Hernández J. et al. (2008) *Astrophys. J.*, *686*, 1195.
Hernández J. et al. (2010) *Astrophys. J.*, *722*, 1226.
Hirose S. and Turner N. J. (2011) *Astrophys. J. Lett.*, *732*, L30.
Hollenbach D. et al. (1994) *Astrophys. J.*, *428*, 654.
Houck J. R. et al. (2004) *Astrophys. J. Suppl.*, *154*, 18.
Huélamo N. et al. (2011) *Astron. Astrophys.*, *528*, L7.
Hughes A. M. et al. (2007) *Astrophys. J.*, *664*, 536.
Hughes A. M. et al. (2009) *Astrophys. J.*, *698*, 131.
Ingleby L. et al. (2009) *Astrophys. J. Lett.*, *703*, L137.
Ingleby L. et al. (2011) *Astrophys. J.*, *743*, 105.
Ingleby L. et al. (2012) *Astrophys. J. Lett.*, *752*, L20.
Ingleby L. et al. (2013) *Astrophys. J.*, *767*, 112.
Ireland M. J. (2012) in: *Society of Photo-Optical Instrumentation Engineers (SPIE) Conference Series*, vol. 8447 of *Society of Photo-Optical Instrumentation Engineers (SPIE) Conference Series*.
Ireland M. J. and Kraus A. L. (2008) *Astrophys. J. Lett.*, *678*, L59.
Isella A. et al. (2009) *Astrophys. J.*, *701*, 260.
Isella A. et al. (2010a) *Astrophys. J.*, *714*, 1746.
Isella A. et al. (2010b) *Astrophys. J.*, *725*, 1735.
Isella A. et al. (2012) *Astrophys. J.*, *747*, 136.
Isella A. et al. (2013) *Astrophys. J.*, *775*, 30.
Jeffries R. D. et al. (2011) *Mon. Not. R. Astron. Soc.*, *418*, 1948.
Jensen E. L. N. and Mathieu R. D. (1997) *Astron. J.*, *114*, 301.
Joy A. H. (1945) *Astrophys. J.*, *102*, 168.
Ke T. T. et al. (2012) *Astrophys. J.*, *745*, 60.
Kim K. H. et al. (2009) *Astrophys. J.*, *700*, 1017.
Kim K. H. et al. (2013) *Astrophys. J.*, *769*, 149.
Klahr H. H. and Henning T. (1997) *Icarus*, *128*, 213.
Kley W. and Dirksen G. (2006) *Astron. Astrophys.*, *447*, 369.
Kley W. and Nelson R. P. (2012) *Annu. Rev. Astron. Astrophys.*, *50*, 211.
Koepferl C. M. et al. (2013) *Mon. Not. R. Astron. Soc.*, *428*, 3327.
Koerner D. W. and Sargent A. I. (1995) *Astron. J.*, *109*, 2138.
Kraus A. L. and Ireland M. J. (2012) *Astrophys. J.*, *745*, 5.
Kraus A. L. et al. (2008) *Astrophys. J.*, *679*, 762.
Kraus A. L. et al. (2011) *Astrophys. J.*, *731*, 8.
Kraus S. (2013) *ArXiv e-prints*.
Kraus S. et al. (2013) *Astrophys. J.*, *768*, 80.
Krautter J. et al. (1997) *Astron. Astrophys. Suppl.*, *123*, 329.
Lada C. J. et al. (2006) *Astron. J.*, *131*, 1574.
Lai D. and Zhang H. (2008) *Astrophys. J.*, *683*, 949.
Lee N. et al. (2011) *Astrophys. J.*, *736*, 135.
Li H. et al. (2005) *Astrophys. J.*, *624*, 1003.
Li H. et al. (2009) *Astrophys. J. Lett.*, *690*, L52.
Liskowsky J. P. et al. (2012) *Astrophys. J.*, *760*, 153.
Lubow S. H. and D'Angelo G. (2006) *Astrophys. J.*, *641*, 526.
Lubow S. H. et al. (1999) *Astrophys. J.*, *526*, 1001.
Luhman K. L. and Mamajek E. E. (2012) *Astrophys. J.*, *758*, 31.
Luhman K. L. et al. (2010) *Astrophys. J. Suppl.*, *186*, 111.
Lynden-Bell D. and Pringle J. E. (1974) *Mon. Not. R. Astron. Soc.*, *168*, 603.
Lyra W. and Lin M.-K. (2013) *Astrophys. J.*, *775*, 17.
Lyra W. et al. (2009) *Astron. Astrophys.*, *493*, 1125.
Maaskant K. M. et al. (2013) *Astron. Astrophys.*, *555*, A64.
Manoj P. et al. (2011) *Astrophys. J. Suppl.*, *193*, 11.
Marcy G. et al. (2005) *Progress of Theoretical Physics Supplement*, *158*, 24.
Marsh K. A. and Mahoney M. J. (1992) *Astrophys. J. Lett.*, *395*, L115.
Marsh K. A. and Mahoney M. J. (1993) *Astrophys. J. Lett.*, *405*, L71.
Martin R. G. and Lubow S. H. (2011) *Mon. Not. R. Astron. Soc.*, *413*, 1447.
Mathews G. S. et al. (2012) *Astrophys. J.*, *753*, 59.
Mayama S. et al. (2012) *Astrophys. J. Lett.*, *760*, L26.
McClure M. K. et al. (2010) *Astrophys. J. Suppl.*, *188*, 75.
McClure M. K. et al. (2012) *Astrophys. J. Lett.*, *759*, L10.
Megeath S. T. et al. (2005) *Astrophys. J. Lett.*, *634*, L113.
Merín B. et al. (2010) *Astrophys. J.*, *718*, 1200.
Monnier J. D. and Millan-Gabet R. (2002) *Astrophys. J.*, *579*, 694.
Morales-Calderón M. et al. (2011) *Astrophys. J.*, *733*, 50.

Morishima R. (2012) *Mon. Not. R. Astron. Soc.*, *420*, 2851.
Muench A. A. et al. (2007) *Astron. J.*, *134*, 411.
Mulders G. D. et al. (2010) *Astron. Astrophys.*, *512*, A11+.
Mulders G. D. et al. (2013) *ArXiv e-prints*.
Muto T. et al. (2010) *Astrophys. J.*, *724*, 448.
Muzerolle J. et al. (2003) *Astrophys. J. Lett.*, *597*, L149.
Muzerolle J. et al. (2009) *Astrophys. J. Lett.*, *704*, L15.
Muzerolle J. et al. (2010) *Astrophys. J.*, *708*, 1107.
Nagel E. et al. (2010) *Astrophys. J.*, *708*, 38.
Najita J. R. et al. (2000) *Protostars and Planets IV*, p. 457.
Najita J. R. et al. (2007a) *Mon. Not. R. Astron. Soc.*, *378*, 369.
Najita J. R. et al. (2007b) in: *Protostars and Planets V*, (edited by B. Reipurth, D. Jewitt, and K. Keil), pp. 507–522.
Najita J. R. et al. (2008) *Astrophys. J.*, *687*, 1168.
Najita J. R. et al. (2009) *Astrophys. J.*, *697*, 957.
Najita J. R. et al. (2010) *Astrophys. J.*, *712*, 274.
Natta A. et al. (2006) *Astron. Astrophys.*, *452*, 245.
Nayakshin S. (2013) *Mon. Not. R. Astron. Soc.*, *431*, 1432.
Oliveira I. et al. (2010) *Astrophys. J.*, *714*, 778.
Olofsson J. et al. (2011) *Astron. Astrophys.*, *528*, L6.
Olofsson J. et al. (2013) *Astron. Astrophys.*, *552*, A4.
Owen J. E. and Clarke C. J. (2012) *Mon. Not. R. Astron. Soc.*, *426*, L96.
Owen J. E. et al. (2010) *Mon. Not. R. Astron. Soc.*, *401*, 1415.
Owen J. E. et al. (2011) *Mon. Not. R. Astron. Soc.*, *412*, 13.
Owen J. E. et al. (2012) *Mon. Not. R. Astron. Soc.*, *422*, 1880.
Paardekooper S.-J. and Mellema G. (2004) *Astron. Astrophys.*, *425*, L9.
Paardekooper S.-J. and Mellema G. (2006) *Astron. Astrophys.*, *453*, 1129.
Papaloizou J. C. B. et al. (2001) *Astron. Astrophys.*, *366*, 263.
Papaloizou J. C. B. et al. (2007) in: *Protostars and Planets V*, (edited by B. Reipurth, D. Jewitt, and K. Keil), pp. 655–668.
Pichardo B. et al. (2005) *Mon. Not. R. Astron. Soc.*, *359*, 521.
Pierens A. and Nelson R. P. (2008) *Astron. Astrophys.*, *482*, 333.
Piétu V. et al. (2005) *Astron. Astrophys.*, *443*, 945.
Piétu V. et al. (2006) *Astron. Astrophys.*, *460*, L43.
Piétu V. et al. (2007) *Astron. Astrophys.*, *467*, 163.
Pinilla P. et al. (2012) *Astron. Astrophys.*, *538*, A114.
Pogodin M. A. et al. (2012) *Astronomische Nachrichten*, *333*, 594.
Pontoppidan K. M. et al. (2008) *Astrophys. J.*, *684*, 1323.
Pontoppidan K. M. et al. (2010) *Astrophys. J.*, *720*, 887.
Qi C. et al. (2011) *Astrophys. J.*, *740*, 84.
Quanz S. P. et al. (2011) *Astrophys. J.*, *738*, 23.
Quanz S. P. et al. (2012) *Astron. Astrophys.*, *538*, A92.
Quanz S. P. et al. (2013a) *Astrophys. J. Lett.*, *766*, L1.
Quanz S. P. et al. (2013b) *Astrophys. J. Lett.*, *766*, L2.
Quillen A. C. and Trilling D. E. (1998) *Astrophys. J.*, *508*, 707.
Rameau J. et al. (2012) *Astron. Astrophys.*, *546*, A24.
Ratzka T. et al. (2005) *Astron. Astrophys.*, *437*, 611.
Ratzka T. et al. (2007) *Astron. Astrophys.*, *471*, 173.
Regály Z. et al. (2010) *Astron. Astrophys.*, *523*, A69.
Regály Z. et al. (2012) *Mon. Not. R. Astron. Soc.*, *419*, 1701.
Rice W. K. M. et al. (2003) *Mon. Not. R. Astron. Soc.*, *342*, 79.
Rice W. K. M. et al. (2006) *Mon. Not. R. Astron. Soc.*, *373*, 1619.
Romero G. A. et al. (2012) *Astrophys. J.*, *749*, 79.
Rosenfeld K. A. et al. (2012) *Astrophys. J.*, *757*, 129.
Rosenfeld K. A. et al. (2013) *Astrophys. J.*, *775*, 136.
Rosotti G. P. et al. (2013) *Mon. Not. R. Astron. Soc.*, *430*, 1392.
Rydgren A. E. et al. (1976) *Astrophys. J. Suppl.*, *30*, 307.
Salyk C. et al. (2007) *Astrophys. J. Lett.*, *655*, L105.
Salyk C. et al. (2009) *Astrophys. J.*, *699*, 330.
Salyk C. et al. (2011) *Astrophys. J.*, *743*, 112.
Salyk C. et al. (2013) *Astrophys. J.*, *769*, 21.
Sicilia-Aguilar A. et al. (2008) *Astrophys. J.*, *687*, 1145.
Sicilia-Aguilar A. et al. (2009) *Astrophys. J.*, *701*, 1188.
Sicilia-Aguilar A. et al. (2011) *Astrophys. J.*, *742*, 39.
Skrutskie M. F. et al. (1990) *Astron. J.*, *99*, 1187.
Stempels H. C. and Gahm G. F. (2004) *Astron. Astrophys.*, *421*, 1159.
Strom K. M. et al. (1989) *Astron. J.*, *97*, 1451.
Takami M. et al. (2013) *Astrophys. J.*, *772*, 145.
Tamura M. (2009) in: *American Institute of Physics Conference Series*, vol. 1158 of *American Institute of Physics Conference Series*, (edited by T. Usuda, M. Tamura, and M. Ishii), pp. 11–16.
Tanaka H. et al. (2005) *Astrophys. J.*, *625*, 414.
Tang Y.-W. et al. (2012) *Astron. Astrophys.*, *547*, A84.
Tanii R. et al. (2012) *PASJ*, *64*, 124.
Tatulli E. et al. (2011) *Astron. Astrophys.*, *531*, A1.
Thalmann C. et al. (2010) *Astrophys. J. Lett.*, *718*, L87.
Tsukagoshi T. et al. (2013) in: *Astronomical Society of the Pacific Conference Series*, vol. 476 of *Astronomical Society of the Pacific Conference Series*, (edited by R. Kawabe, N. Kuno, and S. Yamamoto), p. 391.
Turner N. J. et al. (2010) *Astrophys. J.*, *708*, 188.
Tuthill P. G. et al. (2000) *PASP*, *112*, 555.
Valenti J. A. et al. (1993) *Astron. J.*, *106*, 2024.
van der Marel N. et al. (2013) *Science*, *340*, 1199.
van der Plas G. et al. (2009) *Astron. Astrophys.*, *500*, 1137.
Vicente S. et al. (2011) *Astron. Astrophys.*, *533*, A135.
Weidenschilling S. J. (1977) *Mon. Not. R. Astron. Soc.*, *180*, 57.
Weinberger A. J. et al. (1999) *Astrophys. J. Lett.*, *525*, L53.
Werner M. W. et al. (2004) *Astrophys. J. Suppl.*, *154*, 1.
Whipple F. L. (1972) in: *From Plasma to Planet*, (edited by A. Elvius), p. 211.
White R. J. and Ghez A. M. (2001) *Astrophys. J.*, *556*, 265.
Williams J. P. and Cieza L. A. (2011) *Annu. Rev. Astron. Astrophys.*, *49*, 67.
Wolf S. and D'Angelo G. (2005) *Astrophys. J.*, *619*, 1114.
Wolf S. and Klahr H. (2002) *Astrophys. J. Lett.*, *578*, L79.
Wolk S. J. and Walter F. M. (1996) *Astron. J.*, *111*, 2066.
Zhu Z. et al. (2011) *Astrophys. J.*, *729*, 47.
Zhu Z. et al. (2012) *Astrophys. J.*, *755*, 6.
Zhu Z. et al. (2013) *Astrophys. J.*, *768*, 143.

This 2-column preprint was prepared with the AAS LaTeX macros v5.2.